# The Development and Characterization of Ubiquitin Variants as Molecular Probes of E3 Ligase HUWE1

Angelo Vivona

A Thesis Submitted to the Faculty of Graduate Studies in Partial Fulfillment of the Requirements for the Degree of Master of Science

Graduate Program in Biology
York University
Toronto, Ontario

April 2024

© Angelo Vivona, 2024

# ABSTRACT

Mutations in the ubiquitin E3 ligase HUWE1 (HECT, UBA, and WWE containing protein 1) have been linked to X-linked intellectual disability (XLID). However, the large size of HUWE1 poses challenges for studying the mechanisms and functions of its domains using current technologies. In this study, we employed biochemical and cell-based approaches to characterize two protein-engineered Ubiquitin Variants (UbVs) targeting specific HUWE1 domains. Two UbVs were developed via a collaboration with Dr. Wei Zhang's lab (University of Guelph) to bind to the UBM1 and HECT domains of HUWE1 specifically, and their targeted binding affinities and cross-interactions were investigated. Additionally, the interactions of the HUWE1 protein with both UbVs and a fusion of these two UbVs were further validated in cells. Lastly, the effect of UbVs on endogenous HUWE1 was assessed by comparing HUWE1 substrate levels in the proteasome inhibitor MG132 treated and untreated cells. Our findings reveal that both HUWE1 UbVs interact strongly with their respective targeted domains; both HUWE1 UbVs and the fusion UbV interact with HUWE1 protein and modulate its function in cells. These results suggest that UbVs hold promise as probes for advancing research into the mechanistic and functional aspects of HUWE1.

# ACKNOWLEDGMENTS

I want to express my sincere gratitude to the following people who have helped me and supported me through my journey. Firstly, I would like to thank Dr. **Yi Sheng**, my supervisor. You gave me a chance and provided me with the experience I need to complete this project. Without you, I would not have been able to research such an incredible topic or complete this MSc. Thank you, Dr. Sheng, you have been a major part of my life these last three years. I know we had some disagreements through my project, but through these discussions I have learned so much that has contributed both to my research and towards me personally. I have enjoyed being a part of your lab and even though I would change some things in my experiments with the knowledge I know now, I would never change the experience I had in this lab. Thank you with all my heart for being my supervisor.

I would also like to thank my advisor, Dr. **Dasantila Golemi-Kotra**, for always providing such excellent feedback and thought-provoking questions. I am truly thankful that you agreed to be a part of this journey together with me.

I also would like to express my gratitude to all the members of the Sheng Lab both past and present. To **Gaby**, thank you for helping me and answering my questions whenever I asked. I enjoyed our night TV sessions. To **Daniel**, thank you for always being there for me to talk to, when trying to get through my thoughts. I enjoyed talking and discovering new podcasts with you. I truly enjoyed our time together and will remember those moments forever. To **Nour,** it was a pleasure teaching you, working with you and talking with you, especially during our coffee breaks. To **Rufei, Venessa, Sanjay** and **Nikita,** I am truly happy to have taught and learned science with you. Thank you all in the Sheng lab for being the best lab members a person can ever have. I appreciated every moment.

There are many people that I have made friends with during my time in the Life Science Building. I would like to thank, **David, Nick, Christina, Kyra, Jennifer, Joyce, Suki, Krstina, Serina, Connor, Britney, Sehaj, Sihat, Ivan, Farnaz, Sarah, Gagan, Christine, Arnold** and so much more, for the time, expertise and the friendship that they gave.

To my **dad, Mom, Nonna Libera, Nonna Sina** and my brother, I am truly grateful for my life together with you, and I am so happy you are my family. To my **Nonno Angelo** and **Nonno Salvatore,** you may not be here, but you pushed me to become who I am and to try and find a way to help people. Thank you all for your love and support. I would not be who I am without all of you.

To my wife, **Manami,** I am extremely lucky to have your support with me. You believed in me and are continuing to push me to do better. I am so happy to have met you 5 years ago and experiencing this moment with you today. I love you and can never thank you enough for supporting me throughout this MSc thesis and more.

Finally, to my daughter **Mia,** you appeared in this world during my time here. Looking at you makes me realize repeatedly why I am in this field. Your smile has supported me, and your laugh has gotten me through tough times. Thank you for making this moment even more special.

# Table of Contents

# LIST OF TABLES

# LIST OF FIGURES

# ABBREVIATIONS

**APC/C – Anaphase-promoting complex/cyclosome**

**ARLD - Armadillo-repeat-like domain**

**BioID – proximity-dependent biotin identification**

**BLI – BioLayer Interferometry**

**BRISC - Brcc36-containing isopeptidase complex**

**Co-IP – Co-immunoprecipitation**

**Cryo-EM – Cryo-electron microscopy**

**DUB – Deubiquitinating Enzyme**

**E1 - Ubiquitin activating enzyme**

**E2 – Ubiquitin conjugating enzyme**

**E3 – Ub E3 Ligase**

**ENaC - epithelial Na+ channel**

**HCV – Hepatitis C Virus**

**HECT – Homologous to the E6-AP Carboxyl Terminus**

**HU.1 – UbV_HECT_1**

**HUWE1 – HECT, UBA and WWE domain-containing protein 1**

**ID - Intellectual Disability**

**IPTG – Isopropyl b-D-1-thiogalactopyranoside**

**NEM - N-Ethylmaleimide**

**NSCLC - Non-small-cell-lung carcinomas**

**OMIM - Online Mendelian Inheritance in Man**

**PCNA - Proliferating cell nuclear antigens**

**PTM – Post-Translational Modification**

**PROTAC – Proteolysis-targeting chimeras**

**RBR – RING1-IBR-RING2**

**RING – Really Interesting New Gene**

**tUBM – tandem Ubiquitin Binding Motif**

**Ub - Ubiquitin**

**UBA – Ubiquitin-Associated**

**UBM – Ubiquitin Binding Motif**

**UbV – Ubiquitin Variant**

**UbV4 – UbV_UBM_4**

**UIM – Ubiquitin Interacting Motif**

**UPS – Ubiquitin Proteasome System**

**USP – Ubiquitin Specific Protease**

**XLID – X-linked Intellectual Disability**

# Chapter 1: Introduction

## 1.1 Protein Engineering by Phage Display

Protein engineering is a process that involves the deliberate design and creation of proteins with highly specific functions. Protein engineering harnesses the power of DNA manipulation, encompassing techniques such as nucleotide substitution, insertion, and deletion, to add precise changes to protein sequences that align with particular functions.

One example of protein engineering is phage display technology introduced by George Smith and Gregory Winter during the 1980s and 1990s. They utilized bacteriophages, viruses that infect bacteria, to engineer an array of bacteriophage-bound proteins, which enables the identification and selection of proteins from the phage display library with exceptional specificity towards predefined targets (Smith et al., 1998). With the rapid advancement of this technology, phage display offers rich opportunities for applications ranging from molecular probes to clinical diagnostics. In this literature review, the principles of phage display technology will be explored, alongside a discussion of its diverse applications, providing essential context for understanding its relevance to this thesis.

### 1.1.1 Phage Display Library Screening

Phage display involves the presentation of foreign proteins or peptides on the surface of filamentous bacteriophage. This allows for selection or engineering of proteins with specific functions. The approach can be divided into two steps (Fig 1.1). (1) Library creation: A phage library is generated by fusing different protein or peptide variants with a pIII protein, a structural protein found on the surface of filamentous bacteriophage. A good bacteriophage library contains a vast number of different variants, making it a valuable resource for protein engineering and selection. (2) Biopanning: The variant library goes through a screening process known as

biopanning. Biopanning identifies specific protein or peptide variants binding to target molecules by incubating the display library proteins or peptides with an immobilized target and removing the non-bound phages via washing. Incubating and washing are done in several cycles, and the remaining bound phages are then eluted, amplified, and sequenced (Wu *et al.*, 2016). This allows identification of proteins or peptides with desired properties. This technology offers a rapid and convenient means to generate novel engineered proteins, including engineered antibodies, enzymes, and therapeutical proteins (Koellhoffer *et al*., 2012; Ponsard *et al.,* 2001; Weinblatt *et al*., 2003).

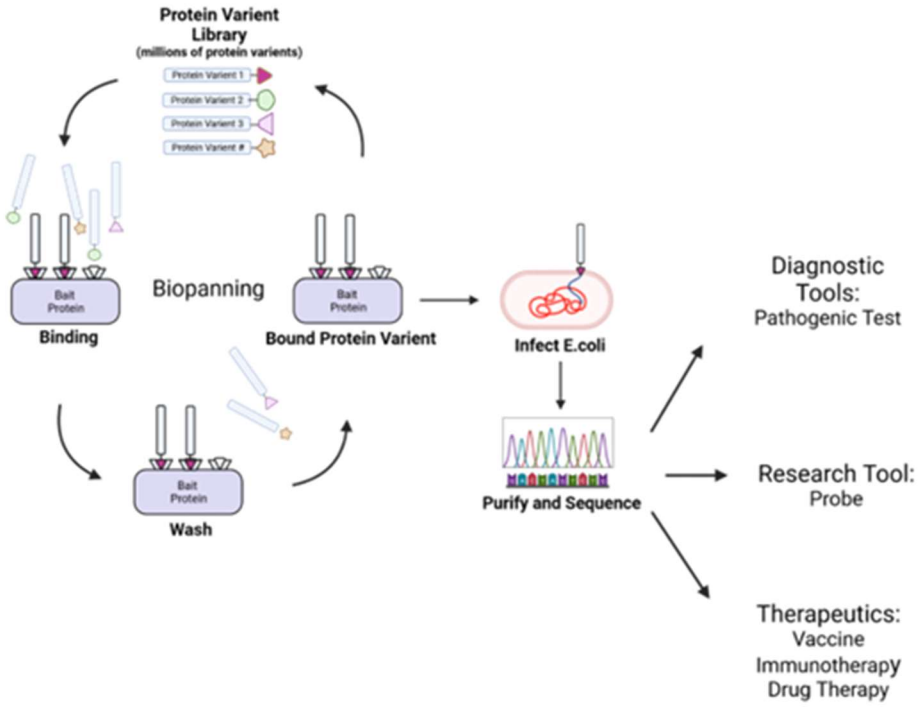


**Figure 1.1: Schematic of Phage Display Screening**
Illustration depicting the process of the phage display library screening. The process begins with presentation of diverse protein variants on the surface of bacteriophages to create a phage display library. These variants are then exposed to a bait protein. The non-bound variants are washed away. The bound protein bacteriophage is used to infects *E. coli* to be amplified and identified by sequencing (Wu *et al.,* 2016)

Phage display has emerged as a versatile and invaluable tool with diverse biomedical research and therapeutic applications. One notable biomedical application of phage display is epitope mapping. An epitope is a region on the antigen that can be recognized by an antibody. During pathogenic infections, the host immune system generates B and T cells targeting foreign epitopes from the pathogen. Epitope mapping using peptide phage libraries can identify the peptide sequence of antigenic epitopes recognized by immune cells. The utilization of phage display in epitope mapping has been employed for pathogen targeting or as a rapid diagnostic method to identify pathogens.

One such application using peptide-based phage display is mapping pathogenic hepatitis C virus (HCV) epitopes for viral detection and vaccine development. Originally, HCV was detected via the presence of anti-HCV antibody in infected individuals induced by HCV viral protein. Researchers utilized phage display to identify and develop peptide mimics that contain the viral epitope sequence (Prezzi *et al.*, 1996). Such phage-display-HCV peptide mimics could be used to detect HCV infection by binding to an individual's anti-HCV antibody, providing a quick and accessible diagnostic tool. In addition, these HCV mimics showed potential for vaccine development. Research showed these HCV mimics can be used to induce a specific immune response against HCV in mice similar to that induced by the native virus (Prezzi *et al., 1996)*. This underscores the capacity of phage display technology as a desirable strategy to augment the development of vaccines and immunotherapy. Similar phage display screening approaches have been used to select disease-specific antigens, cell-specific peptides and organ-specific peptides, expanding its potential applications in diagnostics and therapeutics (*Chen* et al., 2007; Wu *et al.,* 2001).

## 1.2 Ubiquitin Variants (UbVs)

Researchers have broadened the capability of this technology through creation of phage display libraries comprising of protein variants. The protein-based phage display introduces diversity on the protein surface while preserving the stability of the protein scaffold. An example is the FDA-approved therapeutic antibody, adalimumab (Humira), a humanized tumor necrosis factor α (TNFα) antibody. The development of Adalimumab utilized a protein-based phage display library, which employed a human antibody as the protein scaffold with a highly diverse variable region. Applying procedures similar to what were described for the peptide phage display, researchers used biopanning to selectively identify a high-affinity humanized antibody variant targeting the tumor necrosis factor α, ultimately leading to the creation of Adalimumab (Kempeni, 1999). Following this strategy, eight other humanized antibodies were developed against different drug targets and later approved by FDA (Reviewed by Lu et al., 2020).

In 2013, Ernst and colleagues developed a phage display library using ubiquitin as the protein scaffold. Ubiquitin (Ub) is a 76-residue thermostable small protein. It acts as a stable scaffold while multiple mutations are introduced across the protein surface. This phage display library currently contains millions of variants of the Ub protein (UbV), which can be used to screen for specific protein binders against different target proteins (Ernst et al., 2013)

Ernst and colleagues first applied the UbV library to 58 human Ub-specific proteases (USPs), the largest protein family of the deubiquitinating enzymes. The USPs are cysteine proteases with the primary function in removal of Ub from different ubiquitinated substrates (Ernst et al., 2013). Despite their sequence diversity, these USPs share a structurally conserved catalytic

domain comprising a catalytic triad with conserved cysteine, histidine and aspartate residues in the active site (Soboleva & Baker, 2004).

While specific inhibitors for individual USPs are not readily available due to the high degree of structural similarity of the active sites among the USP family members, Ernst and colleagues were able to develop specific UbVs that target USP8, USP21, USP2a using the UbV phage library. UbV specificity results from amino acid modifications of exposed surface regions across its Ub scaffold, which have been demonstrated to affect both binding specificity and affinity to various members of the USP family. By increasing the binding area and affinity of the interface between the individual USPs and the respective UbV, the identified UbVs demonstrated potent inhibition of their respective targets. The UbVs for USP8, USP21, and USP2a showed IC50 values ranging between 2.4 and 25 nM and exhibited no cross-reactivity with other USPs. The mechanism underlying UbV-mediated inhibition of USPs was elucidated through a study on USP15-specific UbV. As a competitive inhibitor, UbVs bind to the canonical Ub-binding site of USP15, locking its catalytic triad in an inactive conformation (Teyra et al., 2019). Building upon these findings, Ernst and colleagues subsequently screened UbVs for two other deubiquitinating enzyme families, known as OTU and JAMM (Ernst et al., 2013; Tencer et al., 2016). As a result, they identified specific UbVs for OTUB1 and Brcc36-containing isopeptidase complex (BRISC). This expanded the repertoire of UbVs targeting deubiquitinating enzymes.

In another study by Zhang et al., UbV phage display was utilized to target another family of Ub-associated proteins, Ub E3 ligases (E3). This family of proteins are involved in virtually every cellular process of eukaryotic cells, and their deregulation is implicated in many diseases and disorders. Zhang et al. conducted a large-scale UbV phage display screening against 28 human and 5 yeast HECT E3 ligase. This screening resulted in the identification of 69 UbVs that

selectively bind to 19 human and 1 yeast E3 ligases (Zhang et al., 2016). Among these UbVs, some inhibit their respective E3 ligase by hijacking the E2 binding site of the catalytic HECT domain and blocking the Ub transfer (Fig 1.2). Additionally, several UbVs were found to be activators of the target E3 ligases, but the exact mechanisms are not well understood. One UbV inhibits polyubiquitination the WWP1 HECT E3 ligase by binding to an exosite, a secondary Ub binding site of the HECT domain, to activate monoubiquitination processivity of the enzyme (Zhang et al., 2016) (Fig 1.2). Using the same strategy, UbV phage display screening was applied to target other type E3 ligases and Ub associated proteins. Since it is still ongoing research, many of the identified UbVs await further characterization.

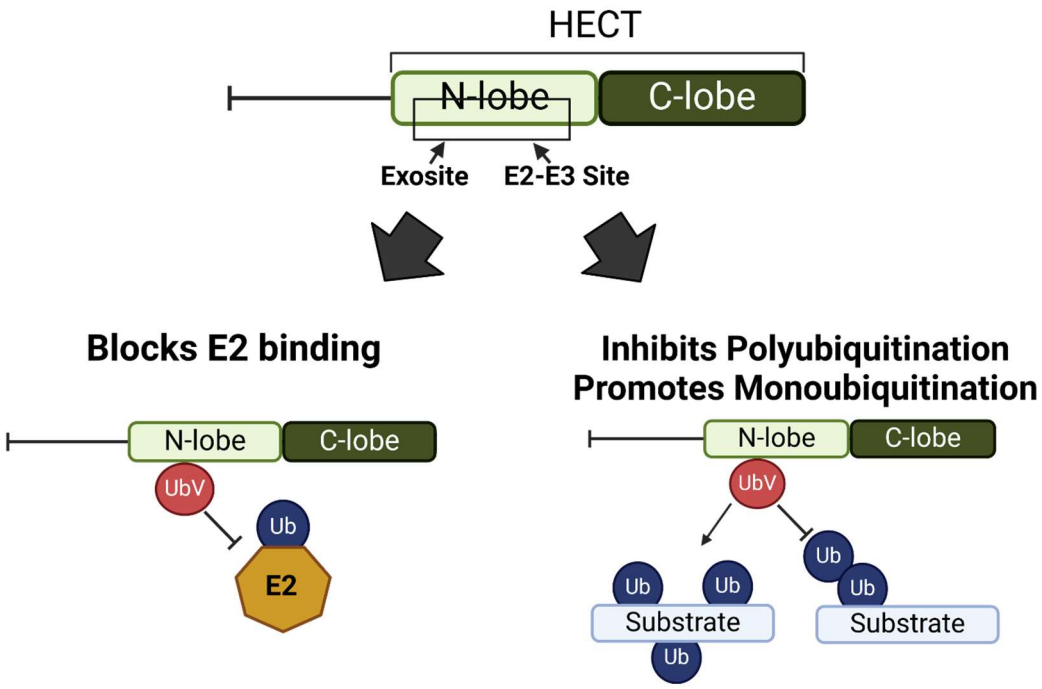


**Figure 1.2: Modulatory effects of UbV on HECT E3 Ligases**
UbV blocks the interaction site between E2 and E3, stopping the transfer of Ub. Alternatively, UbV promotes subsequent monoubiquitination, by blocking the polyubiquitin exosite (Image adapted from Zhang *et al.*, 2016) (Created with BioRender).

At present, UbVs primarily serve as research tools, such as biochemical probes. One study used a UbV that binds the RING domain of the RING E3 ligase anaphase-promoting complex/cyclosome (APC/C) to elucidate the catalytic mechanism of APC/C. APC/C mediates Ub-associated degradation of the cyclins to promote the transition from metaphase to anaphase; however, how the E3 catalytically assembles Ub chains on the cyclins is not clear. Mimicking the structure of Ub, UbV enables visualization of the APC/C RING~E2~Ub complex through cryo-electron microscopy (cryo-EM). The high affinity of the UbV: RING interaction helped anchor the E2~APC/C RING~Ub intermediate, which is challenging to capture through standard techniques due to the weak and transient nature of the complex. This study provides insight into the mechanism underlying APC/C mediated ubiquitination of cyclin and other cell cycle regulators (Brown et al., 2016).

Researchers also explored UbVs as therapeutic agents. A group of researchers used UbVs to develop modulators of NEDD4L, a HECT E3 ligase for an epithelial Na+ channel (ENaC). The deregulation of ENaC activity is directly associated with Liddle syndrome, a hereditary hypertension disorder. Their findings revealed that the NEDD4L-specfic UbVs could regulate the stability and the levels of ENaC in tissues through modulation of NEDD4L function (Zhang et al., 2016).

In summary, UbVs have been used in multiple applications, serving as both research tools for discovering unknown mechanisms or as potential therapeutic agent for diseases associated with Ubiquitin Proteasome System (UPS). To better understand the role of UbV in UPS, the UPS pathway and its components will be discussed in the next section.

### 1.3 Ubiquitin Proteasome System (UPS):

UPS is a regulatory system that controls a variety of cell functions, such as DNA repair, stress responses, cell proliferation, and apoptosis (Reviewed by Deng et al., 2020). UPS includes two major connected components: Ub-mediated protein signalling and proteasome-mediated protein degradation.

#### 1.3.1 The Process of Ubiquitination

Ub-mediated protein signalling starts from protein ubiquitination, a process that conjugates Ub onto target proteins. Ubiquitination involves a reversible ATP-dependent multi-step reaction. The process consists of three enzyme steps (Ciechanover & Schwartz, 1998). The first enzyme, Ub activating enzyme (E1), catalyzes ATP-dependent formation of the E1~Ub intermediate via a thioesterification reaction (Pickart & Eddins, 2004). Next, E1 recruits the Ub conjugate enzyme (E2) and transfers Ub via a thioester linkage. Finally, the Ub ligase enzyme (E3) facilitates covalent attachment of Ub onto a substrate via a peptide bond (Reviewed by Gui et al., 2021). The process can be reversed by deubiquitinating enzymes (DUBs) such as USPs, which remove Ub from the ubiquitinated substrates through a hydrolysis reaction (Reviewed by Wolberger, 2014) (Fig 1.3A).

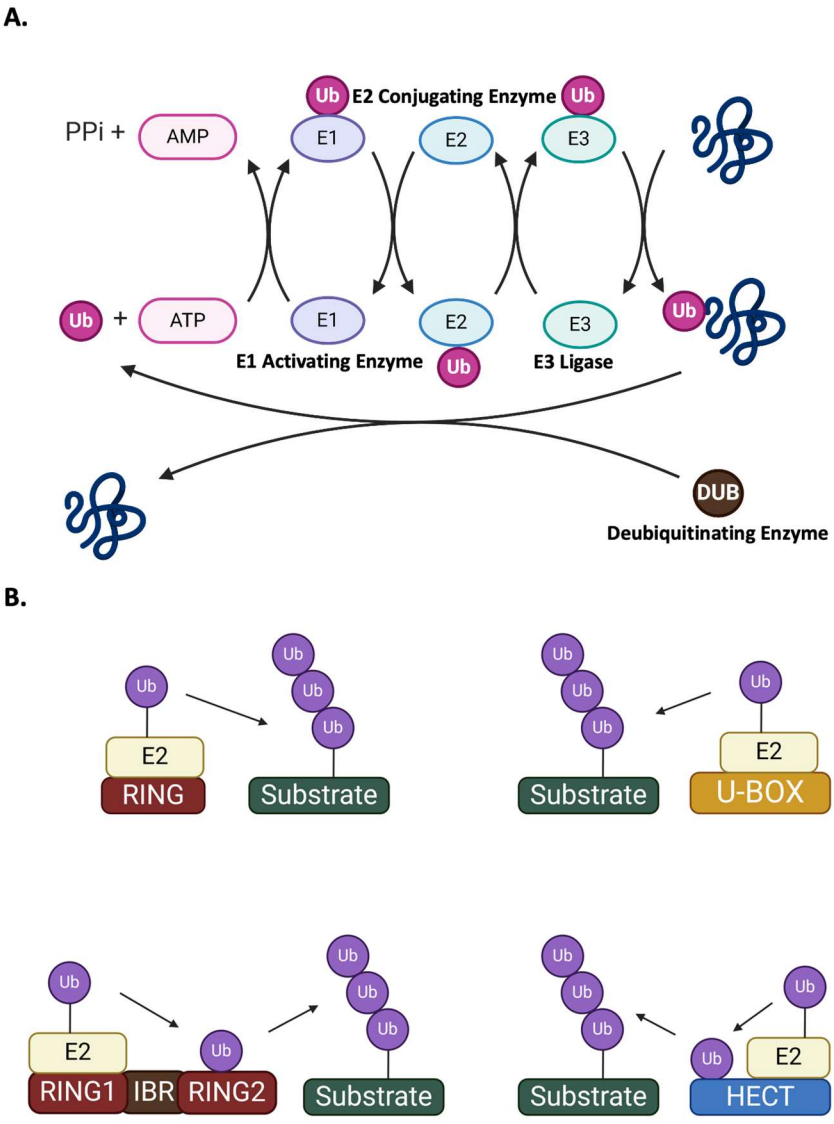


**Figure 1.3: Schematic of the Ubiquitin Proteasome System Process**

A) schematic drawing of the UPS process. The Ub is activated by E1 through an ATP-dependent reaction. The Ub then is transferred through E2 and conjugated on the substrate protein by E3. 26S proteasome interacts with the Ub attached substrate protein resulting in protein degradation. DUB can reverse the process by removing Ub from the ubiquitinated substrate. B) Top left: RING E3 ligases interact with E2~Ub and transfers the Ub straight from the E2~Ub to the substrate. Top right: U-box E3 Ligases interacts with E2~Ub and transfers the Ub straight from the E2~Ub to the substrate. Bottom left: RBR E3 Ligase transfers the Ub from the E2~Ub intermediate to the catalytic cysteine on RING2 and then transfers it onto the substrate. (bottom right) HECT E3 Ligases transfer the Ub onto the HECT domain catalytic cysteine before conjugating it onto the substrate. (Created with BioRender)

When a single Ub is attached to a substrate, it is termed monoubiquitination. A prominent example is histone H2A monoubiquitination, which signals gene silencing through chromatin modification (Srivastava et al., 2017). On the other hand, polyubiquitin chains are composed of multiple Ub molecules linked in a linear or branched polymer (Reviewed by Van Wijk et al., 2019). Polyubiquitin can be connected with different internal lysines (K6, K11, K27, K29, K33, K48, K63) of Ub or N-terminal methionine, giving rise to linkage specific Ub chains. Different forms of polyubiquitination cause specific cell signalling (Ikeda & Dikic, 2008). For example, K48 homotypic chains and K48-K11 heterotypic chains are associated with degradation by the 26S proteasome (Boughton et al., 2020). In contrast, other linkage types (K6, K33, and K63) are linked with non-degradative functions, such as DNA damage repair, autophagy, and immune response (Reviewed by Van Wijk et al., 2019).

In humans, there is one canonical E1 that activates Ub, approximately forty E2s (Pruneda et al., 2011), and several hundreds of E3 ligases that participate in the ubiquitination process (Toma-Fukai & Shimizu, 2021). E2 enzymes contribute to the linkage specificity of the Ub chains. For example, UBC13 (also known as UbE2N) and UbE2V work together to catalyze K63-linked polyubiquitination, whereas UbE2K generates K48-specific Ub-linkage (Stewart et al., 2016). Conversely, E3 ligases are responsible for recognizing different substrates and catalyzing the Ub-substrate conjugation (Toma-Fukai & Shimizu, 2021). E3 ligases play a critical role in substrate-specific ubiquitination. Mutation and dysfunction of E3 ligases could lead to diseases including, neurodegenerative disorder and cancers (Reviewed by George et al., 2018). Pertaining to this thesis, the functions of different types of E3 ligases will be discussed in the next section.

### 1.3.2 Ubiquitin E3 Ligases

Dependent on their catalytic domains, E3 ligases are categorized into four different types: Really Interesting New Gene (RING), U-box, Ring-Between-Ring (RBR) or Homologous to E6-AP Carboxyl Terminus (HECT) (Reviewed by Yang et al., 2021). These four types use different mechanisms to transfer Ub from E2 and to catalyze Ub-substrate conjugation, as described below.

**RING and U-Box E3 Ligases**

The RING E3 ligases contain a RING domain that facilitates ubiquitination. RING domain binds directly to the E2~Ub complex and transfers Ub directly to the E3-bound substrate via a nucleophilic attack. Furthermore, many RING E3 ligases have additional sites for Ub binding, which is important for processivity of polyubiquitination (Brzovic et al., 2006) (Fig 1.3B).

U-Box E3 ligases are structurally different from RING E3 ligases. However, U-Box E3 ligases share a similar mechanism as RING E3 ligases, in which both bind E2~Ub complex and facilitate Ub transfer and conjugation to the lysine site of the substrates (Reviewed by Yang et al., 2021) (Fig 1.3B).

**RING-IBR-RING (RBR) E3 Ligases**

The catalysis of the RBR E3 ligase requires three domains, RING1-IBR (in-between RING)-RING2. RING1 contains an E2 binding site for recruiting the E2~Ub complex, while IBR-RING2 contains the active site with a catalytic cysteine residue. Although the catalysis of RBR involves RING domain as other RING E3 ligases, its ubiquitination mechanism differs from RING and U-box domains. RBR-mediated ubiquitination is a two-step reaction. In the first step, RING1 binds to the E2~Ub complex, bringing it closer to the active site on IBR-RING2. Then, RING1 transfers the Ub to the catalytic cysteine residues in RING2 and releases the E2. In the second step,

RBR covalently attaches the Ub onto the lysine sites of the substrate (Wang et al., 2023) (Fig 1.3B).

**HECT E3 Ligases**

HECT E3 ligases are named after their conserved HECT domain. The HECT domain contains two lobes, the N-lobe and C-lobe, connected by a flexible link. The N-lobe harbours the E2 binding site, while the C-lobe contains the ubiquitin binding site and a catalytic cysteine for receiving the activated Ub (also known as the donor Ub) from the E2. Similar to RBR E3 ligase, HECT E3 ligase mediated ubiquitination involves two steps: in the first step, the E2~Ub complex binds to the N-lobe, while the Ub on the E2~Ub complex interacts with the C-lobe (Fig 1.3B). This enables E3 to conform around the E2~Ub complex and facilitate Ub transfer to the catalytic cysteine. In the second step, the E3 ligase brings the substrate close to the catalytic cysteine, promoting Ub transfer and conjugation onto the substrate (Lorenz, 2017) (Fig 1.3B).

Some HECT E3 ligases contain a secondary Ub binding site, known as Ub exosite, located on the N-lobe (Fig 1.2, 1.4). This exosite has been shown to regulate the processivity of E3 ligases during ubiquitination, influencing their ability to elongate the Ub chain. Mutations in the Ub exosite have been shown to impair polyubiquitination (Kim et al., 2011; French et al., 2009; Ogunjimi et al., 2010; Kathman et al., 2015).

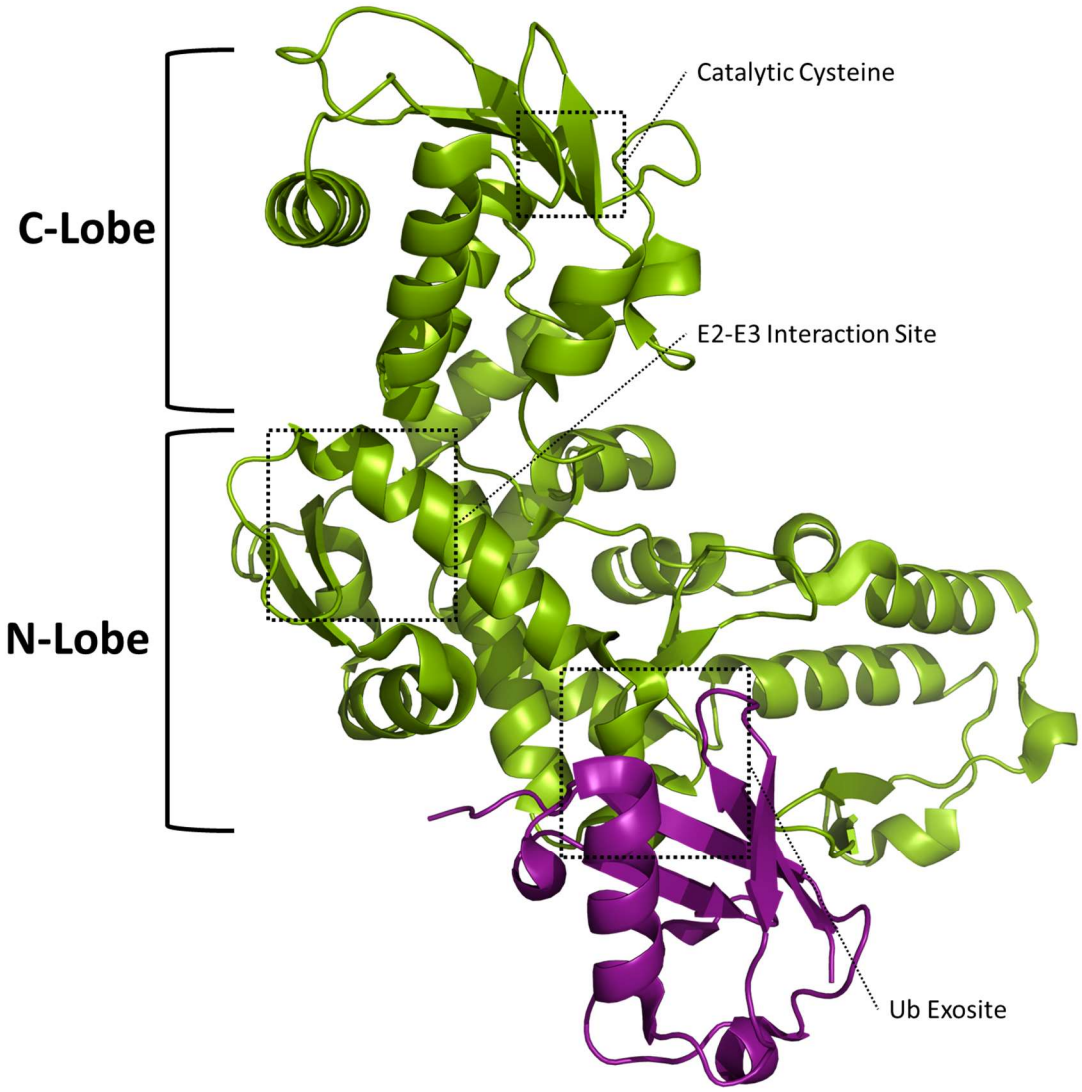


**Figure 1.4: The Cartoon Representation of the HECT Domain of a HECT E3 Ligase**

The HECT domain of NEDD4 E3 ligase (green) (PDB:2XBB) in complex with Ub (purple). The model shows a secondary binding site which Ub interacts with, outside of the normal E2-Ub:E3 interaction site. The Ub secondary binding site (boxed area), exosite at the N-lobe (Lorenz, 2017)

A recent study on WWP1 HECT domain using UbV revealed new insights into the role of this Ub exosite. UbV (P2.3) was first developed as a specific binder for the HECT domain Ub exosite of WWP1 E3 ligase. Interestingly, when UbV (P2.3) binds to the exosite, it greatly

increases the amount of substrate being monoubiquitinated on multiple sites. By blocking the interaction between the E3 and the substrate-linked distal Ub, UbV (P2.3) promotes repeated cycles of substrate ubiquitination (Fig. 1.2). Therefore, the exosite serves as a decisive factor for the type of ubiquitination, i.e. monoubiquitination vs polyubiquitination (Zhang et al., 2016).

### 1.3.3 Ubiquitin Binding and Signal Transduction

Ub binding plays an important role in the ubiquitination process. Apart from the Ub binding sites present in proteins directly involved in ubiquitination, many effector proteins also possess Ub-binding domain/motifs (UBDs). These UBD containing effector proteins are associated with a variety of functions, including protein degradation, endocytosis, pathway activation, DNA repair and more (Reviewed by Dikic et al., 2009). UBDs provide these proteins with the ability to detect the Ub signals through specific Ub(s):UBD interactions.

Based on the structural folds found in UBDs, UBDs are classified into five types: α-helix, zinc finger, PH domain, UBC-like, and Others. While all UBDs bind Ub, some UBDs can detect specific Ub-linkages. For example, DNA polymerase iota contains two copies of UBD domains. Researchers determined that DNA polymerase iota UBD domains bind monoubiquitinated or K63-linked polyubiquitin, but not K48-linked substrates (Burschowsky et al., 2011). This interaction allows DNA polymerase iota to interact with ubiquitinated proliferating cell nuclear antigens (PCNA) and transduce Ub signals for DNA damage repair.

UBD-mediated Ub signalling is also involved in the activation of NF-κB, a master transcriptional factor that induces the inflammation response. Dysregulation of NF-κB has been associated with autoimmune diseases and cancers (Park & Hong. 2016). Proinflammatory cytokines such as TNF-α activate TLR receptor which recruits TRAF6, a RING E3 Ligase. TRAF6

forms K63-linked polyUb chain through autoubiquitination. The K63-linked chain acts as a platform to engage two kinase complexes TAB2/TAK1 through the zinc finger UBD located on the subunit TAB2 and the IKK complex (NEMO/IKKa/IKKb) through UBD domain of the IKK subunit NEMO (Wertz & Dixit, 2010; Laplantine et al., 2009). The recruitment of IKK and TAB2/TAK1 complexes allows the TAK1 kinase to phosphorylate IKK. The phosphorylation promotes IKK kinase activity to phosphorylate the NF-κB inhibitor IκB (Kanayama et al., 2004). This leads to K48-mediated ubiquitination and subsequent degradation of IκB via the β-TRCP E3 ligase (Wertz & Dixit, 2010) and consequently release of NF-κB from IκB inhibition (Fig 1.5). Importantly, the interactions of UBD-Ub play a vital role in this pathway and research has found that mutations that disrupt the UBD-Ub binding abolishes NF-κB activation.

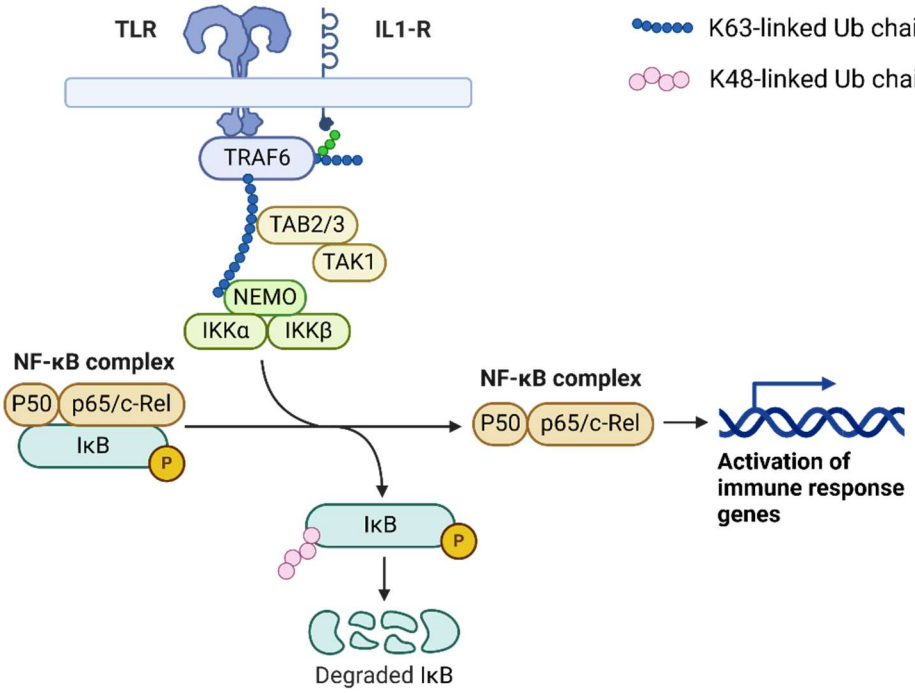


**Figure 1.5: Diagram of the NF- κB pathway**

A schematic drawing of the NF-κB pathway. After TLR activation ubiquitination occurs TRAF6 K63-linked chains anchor TAB2 and NEMO via UBD interaction which promotes phosphorylation on IκB, signalling K48-linked ubiquitination and K48-linked ubiquitinated degradation (Created with Biorender)

Since UBD plays such a prominent role in the cell, UbVs could be used to better understand the interactions of UBD-containing proteins in the diseases associated pathways. Researchers have developed a panel of UbVs to target 42 out of 60 of the predicted Ub-interacting motifs (UIMs), a type of UBD domains with an α-helix structure. Previous research showed that UIM-containing proteins play roles in various cellular functions and are associated with multiple diseases. Therefore, a toolkit of UbVs was created for UIMs and used to understand the function of these UIMs. One of these UbVs targets the single UIM within the cancer-associated DUB, USP28. Researchers used this UbV to probe the mechanism of USP28. DUBs usually mediate Ub cleavage through the interaction of both the proximal Ub (the Ub closer to the substrate) and distal Ub. The researchers tested whether the UIM domain helps USP28 bind to the proximal Ub. By blocking the UIM binding to proximal Ub, this UbV inhibits USP28 cleavage of its polyubiquitinated substrates (Veggiani et al., 2022). Therefore, UbVs can be used to explore the roles of different UBDs in Ub signal transduction and their functions in different cellular processes.

### 1.4 Development of UbVs targeting the HECT E3 ligase HUWE1

A panel of UbVs have been developed to target the HECT domain of multiple human E3 ligases since 2016 (Zhang et al., 2016). Although a large panel of UbVs were developed, research has focused more on UbVs for the NEDD-like family of E3 ligases (i.e. WWP1/2, NEDD4L, NEDD4, SMURF1/2). The functions of the many HECT E3 UbVs have yet to be thoroughly studied. This study focuses on characterization of the UbVs targeting the HECT E3 ligase, known as HECT, UBA, and WWE domains containing E3 ubiquitin ligase 1 (HUWE1).

HUWE1 functions in multiple cellular processes by ubiquitinating various substrates (Reviewed by Kao et al., 2018). HUWE1 regulates apoptosis, DNA damage repair, and gene expression through modulating the function of its substrates, including the tumour suppressor p53,

DNA repair polymerase β, and the transcriptional factor Myc (Leszczynska et al., 2015; Atsumi et al., 2015; Zhao et al., 2009; Qi et al., 2012). Furthermore, HUWE1 plays a critical role in neurodevelopment. Its activity inhibits neuronal proliferation by mediating Ub-proteosome associated degradation of N-Myc, a neural transcriptional factor critical for cortical progenitor proliferation (Zhao et al., 2009). Similarly, HUWE1 activity is required for proper differentiation of cerebellar granule neuron progenitors through Ub-proteasome mediated degradation of Atoh1, the transcriptional factor in the Sonic hedgehog pathway (Forget et al. 2014).

The *HUWE1* gene resides on the X chromosome at gene locus Xp11.22 (Moortgat et al., 2018). It encodes for a polypeptide of ~480 kDa, composed of 4374 amino acids. In 2021, researchers reported that the Cryo-EM 3D structure of the full-length HUWE1 is a solenoid-shaped protein. HUWE1 comprises multiple domains, from N to C terminus, including ARLD1-4, WWE, BH3, UBA, UIM, tUBM and HECT (Fig 1.6). ARLD1-4 serves as the scaffolding that forms the ring-shaped solenoid (Hunkeler et al., 2021). Additional functional domains, including the HECT domains, are tethered to the solenoid ring. The WWE domain is a poly-ADP-ribose (PAR) binding module for interactions with PAR-modified substrates. The BH3 domain binds to the Bcl-2 homology motifs containing proteins, such as Mcl-1 (Hunkeler et al., 2021). HUWE1 contains three sets of UBDs, separated into two Ub binding modules. UBA and UIM form Ub binding module 1 that interact with ubiquitinated substrates (Fig 1.6). Three tandem UBM (tUBM) forms Ub binding module 2. Although also a UBD, the role of the tUBM in HUWE1 requires further study. Lastly, the HECT domain acts as the catalytic domain for ubiquitination process.

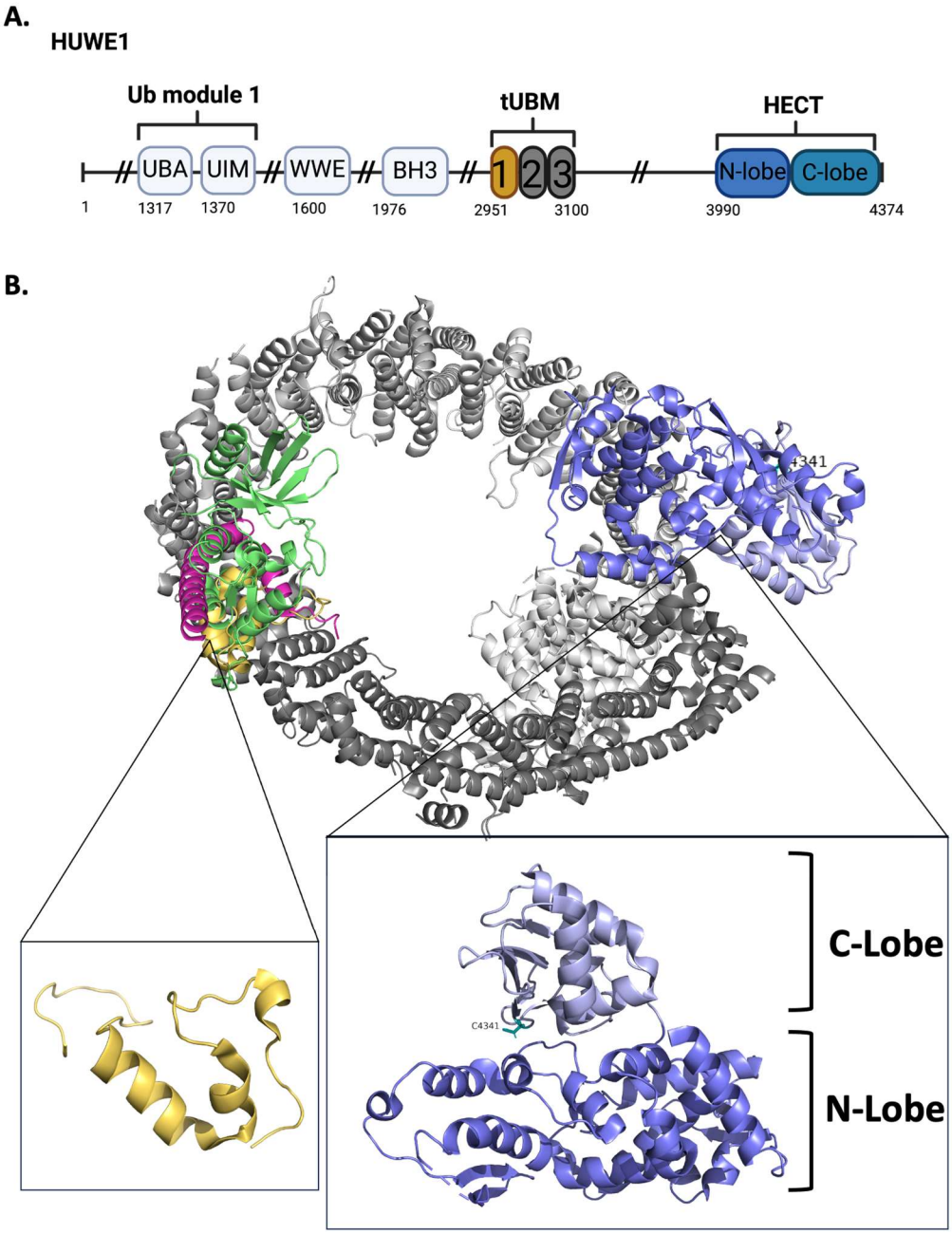


**Figure 1.6: The Structure of E3 ligase HUWE1**

A) Schematic of the HUWE1 domains. B) A Cryo-EM structure of HUWE1 (7MWD) depicted in a ribbon diagram below, containing multiple domains including ARLD1-4 (grey), WWE module (WWE: Orange, HWA: Green and Tower: Magenta). The HECT domain is in blue. tUBM1 is missing from the Cryo-EM structure. The solution structure of its first UBM (PDB:2MUL) is displayed in yellow in the left box. The HECT domain N-lobe, C- lobe, and the Cysteine site (C4341) in cyan are displayed in the right box. The HUWE1 structure was prepared with PyMol.

In the Online Mendelian Inheritance in Man (OMIM) database, *HUWE1* gene mutations have been categorized as one of the genetic causes for the neurodevelopmental disease X-linked Intellectual Disorder (XLID). Several clinical studies of familial XLID patients have identified point mutations, duplications and deletions within the *HUWE1* gene (Moortgat et al., 2018). These XLID patients showed intellectual disability along with distinct facial appearances, such as bifrontal narrowness and thin upper lip, collectively known as Brookes syndrome and J-M syndrome. These syndromes are associated with six *HUWE1* mutations found within two functional domains, tUBM and HECT (Friez et al., 2016). Two mutations were found within the first UBM of the tandem UBM region (R2981H, R3070C) (Moortgat et al., 2018). The other four mutations were found within the HECT domain (R4013W, R4063Q, R4187C, and G4310R) (Friez et al., 2016).

To better understand the functions of these two domains of HUWE1, UbVs were developed through the collaboration with Dr. Wei Zhang's lab (University of Guelph), to target the tUBM and HECT domains. UbV (HU.1) was developed to bind to the HUWE1 HECT domain. UbV UbV4 was developed to bind to the first UBM of the HUWE1 tandem UBM domain covering the XLID mutations R2981 and R3070 (Fig 1.7). These UbVs provide a starting point in investigating their specificity and function towards the HUWE1 protein.

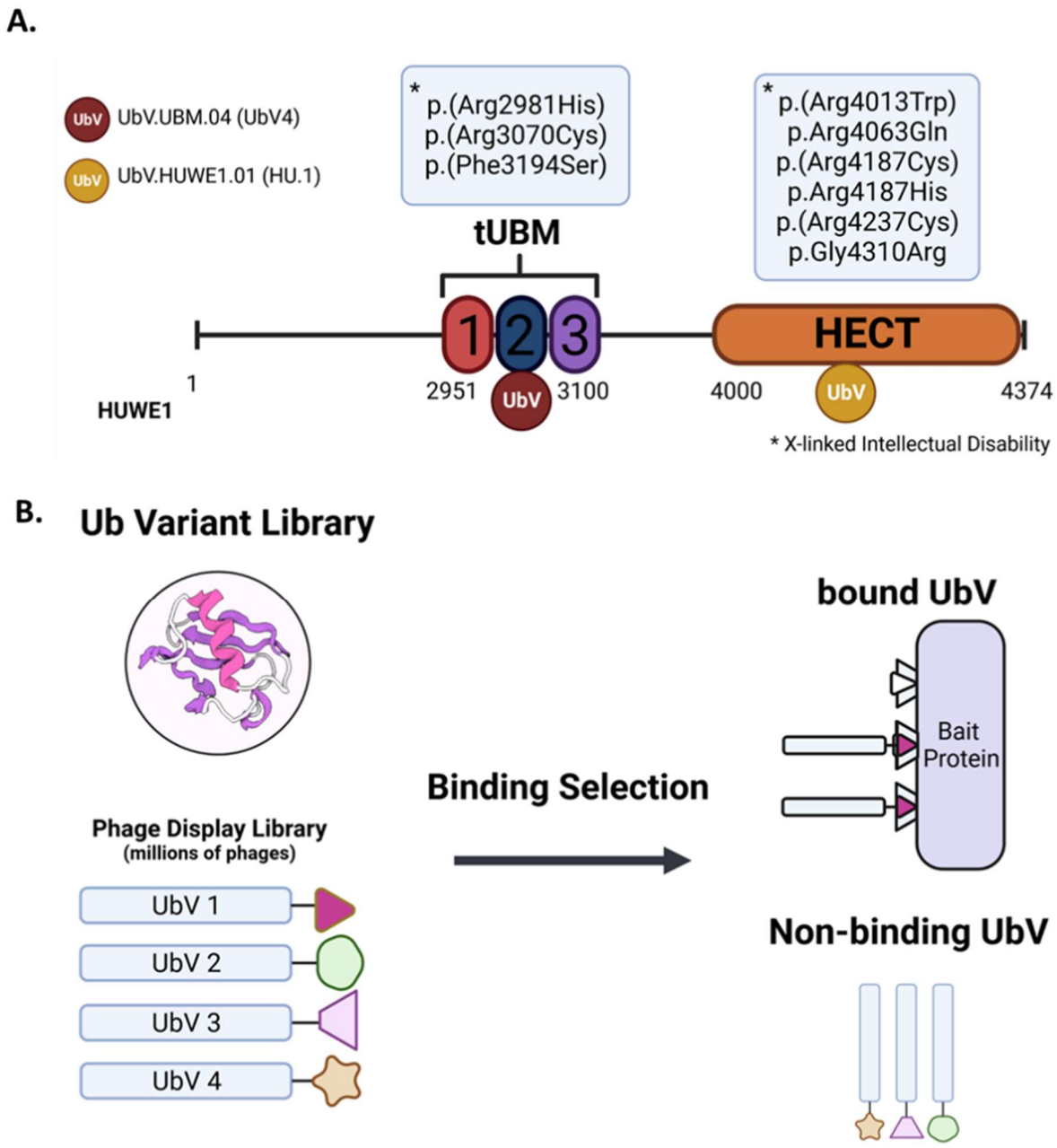


**Figure 1.7: Development of UbV for HUWE1 HECT and tUBM domain using Phage display:**

A) Schematic diagram of the domain architecture of the HUWE1 Domain. Mutations within HUWE1 HECT and tUBM domain that link to X-linked Intellectual disability are displayed (Moortgat et al., 2018). B) A schematic of UbV phage display screening. Within a Ub variant phage display library, each phage presents a unique UbV, which goes through a selection of binding to the protein of interest (Created with Biorender).

## 1.5 Research Objectives

UbVs targeting HECT E3 ligases have been demonstrated to be valuable in both modulating the E3 function, as well as in studying and identifying unknown roles of the HECT E3 ligases in the cell. Although, HUWE1 UbVs were previously developed via collaboration with Dr. Wei Zhang (University of Guelph), these UbVs have yet to be fully understood or utilized. The goal of this study is to better understand the role HUWE1 UbVs play with the HUWE1 E3 ligase. Two specific objectives of this study include: 1) Validate and characterize the UbVs interactions with the HUWE1 domain (UBM and HECT domain). 2) Characterize the effect of UbVs on HUWE1.

To achieve these objectives, this study includes the following four specific sections.

**1: Protein Analysis and Modeling of UbVs:**

A comparison of the HUWE1 HECT UbV 1 (HU.1) and the HUWE1 tUBM UbV, UbV4 was performed and analyzed to determine specific changes in their three regions amino acid sequence and what these changes correspond to compared to wildtype Ub (1UBQ). Further construction modelling was performed via AlphaFold.

**2: Characterization of the bindings of Ubiquitin Variants with the tUBM and HECT domain of HUWE1**

A ubiquitin variant (UbV) has been identified to have a high binding affinity to tUBM via BLI (Biolayer Interferometry). Furthermore, in contrast, the HECT domain (a cis-molecular modulator) is a catalytic ligase for ubiquitin, and another UbV has been demonstrated to bind to the HECT domain. While both HUWE1 UbVs have been developed to specific binding to their domain of interest, research has yet to be conducted on whether the binding is preferential to those

domains or if the UbV has any cross-interaction against other HUWE1 domains. To characterize these UbVs' binding affinities and reveal any cross-interactions, UbV4 and HU.1 were examined and cross-examined with tUBM and HECT via BLI kinetic analysis.

**3: Characterization of UbV binding in mammalian cells (HEK 293T)**

UbV has been recognized to bind to their domains of interest (tUBM and HECT); however, further research has not been conducted against UbV in mammalian cell lines. Since UbV has shown specific binding via BLI, it is hypothesized that both UbVs will interact with the HUWE1 protein. Therefore, UbV interaction with HUWE1 was evaluated in HEK 293T cells. The cells were transfected with FLAG-tagged UbVs and were immunoprecipitated (IP) using FLAG antibody. The IP lysate was immunoblotted for HUWE1 to determine binding.

**4: Characterization of effects UbV on the substrate levels of HUWE1 in HEK 293T cells**

HUWE1 has been demonstrated to mediate and regulate multiple substrates (p53, Myc, β-catenin). Modulation of HUWE1 activity and level can cause changes between these substrates. Therefore, due to binding specificity found in UbV4 and HU.1, it is hypothesized that these UbVs alter and modulate HUWE1 activity. To reveal the impact of UbVs on HUWE1 activity, ubiquitin promotion via MG132 treatment and western blots of HUWE1 substrates (p53 and PARP1 (not published)) were performed to detect changes in HUWE1 function via transfection of HEK 293T cells.

# Chapter 2: Materials and Methods

### 2.1 UbV Protein Sequence Alignment:

The UbV amino acid sequences (HU.1 and UbV4) (DNA sequence provided by the collaborator Dr. Wei Zhang's lab (University of Guelph)) and the Ub sequence derived from the Ub crystal structure (1UBQ) were prepared in FASTA format and used as an input file. Sequences were aligned with the online software Clustal Omega (https://www.ebi.ac.uk/Tools/msa/clustalo/).

### 2.2 Protein structure modeling with AlphaFold

The UbV protein structures were modeled using AlphaFold Colab using the UbV amino acid sequences. The sequences were input into simplified AlphaFold v2.3.2 on Google Colaboratory (https://colab.research.google.com/github/deepmind/alphafold/blob/main/notebooks/AlphaFold.ipynb). All settings and parameters were set to default (Jumper *et al.,* 2021).

### 2.3 Protein Purification

#### 2.3.1 His-tagged UbV Protein expression and purification:

UbVs (HU.1, and UbV4) were purified as His-tagged proteins. To express His-tagged HU.1, and UbV4, pET53 plasmids containing respective genes (Table 2.1) were transformed into E. coli BL21 competent cells. Bacteria were grown in 1L LB media with ampicillin (Cat No. AMP201, BioShop) at a temperature of 37ºC until OD reached between 0.6 – 1. 1 mM IPTG (Cat No. 5820-100G, OmniPur, Isopropyl b-D-1-thiogalactopyranoside) was added to induce the His-tagged UbV protein expression and bacteria were grown at 18ºC overnight before harvest.

His-tagged HU.1, and UbV4 were purified using standard metal affinity purification. Briefly, bacteria were lysed by the lysis buffer (20 mM Tris pH 7.5, 500 mM NaCl, 10% glycerol,

10 mM imidazole, 0.1% Triton x-100, 1 mM benzamidine, 1 mM PMSF) and sonicated using the Sonic Dismembrator Model 500 (2s pulse, 15s off, 25% amplitude, 30 sec, on ice). Next, the solution was centrifuged at 33,708 x g for 30 mins and the supernatant was incubated with the Ni+ resin beads (Cat No. 30210, Qiagen) for 1 hour at 4$^{o}$ C in a rotator. After incubation, the supernatant resin mixture was washed using the wash buffer (20 mM Tris pH 7.5, 500 mM NaCl, 10% glycerol, 20 mM imidazole, 0.1% Triton x-100, 1 mM benzamidine, 1 mM PMSF). The proteins were eluted with the elution buffer (20 mM Tris pH 7.5, 500 mM NaCl, 10% glycerol, 400 mM imidazole, 0.1% Triton x-100, 1 mM benzamidine, 1 mM PMSF). Purified UbVs were run on a 12.5% SDS-PAGE gel and shown as bands of 8.5 kDa (Fig 3.4).

**Table 2.1** A table of the plasmids used for protein purification

| Plasmid Name | Plasmid Type | Description |
|---|---|---|
| UbV_HU.1 (HU.1) | pET53 | A His-tagged plasmid. The UbV sequence was cloned with an N-terminus His tag. The E. coli expression pET53-UbV was provided by the collaborator Dr. Wei Zhang's lab (University of Guelph) |
| UbV4_UBM (UbV4) | pET53 | A His-tagged plasmid. The UbV sequence was cloned with an N-terminus His-tag. The E. coli expression pET53-UbV was provided by the collaborator Dr. Wei Zhang's lab (University of Guelph) |
| HECT (GST-HECT) | pGEX-2KT | A GST-tagged plasmid containing HUWE1 3760-4374 amino acids sequence. The pGEX-2KT-HECT vector was prepared in the Sheng lab from a previous project. |
| UBM1 (GST-UBM1) | pGEX-2KT | A GST-tagged plasmid containing HUWE1 2951-3003 amino acid sequence. The pGEX-2KT-UBM1 vector was prepared in the Sheng lab from a previous project. |

### 2.3.2 GST-tagged HUWE1 Protein expression and purification:

To express GST-tagged proteins, pGEX-2KT plasmids containing HUWE1 UBM1 and HECT respective genes were transformed into E. coli BL21 competent cells. Bacteria were grown in 200 mL LB Media with ampicillin at a temperature of 37ºC until OD reached between 0.6 – 1. 1 mM IPTG was added to induce the GST-tagged protein expression and bacteria were grown at 18ºC overnight before harvest.

GST-tagged proteins (HUWE1 UBM1 and HECT) were purified using Glutathione affinity purification. Briefly, bacteria were lysed by the Lysis buffer (20 mM Tris pH 7.5, 500 mM NaCl, 10% glycerol, 0.1% Triton x-100, 1 mM benzamidine, 1 mM PMSF) and sonicated using Sonic Dismembrator Model 500 (Fisher Scientific) (2s pulse, 15s off, 25% amplitude, 30 sec, on ice). Following centrifugation, the supernatant was incubated with the Glutathione-Sepharose resin beads (Cat No. 10075271, GE Healthcare) for 1 hour at 4º C in a rotator. After incubation, the supernatant resin mixture was washed using the wash buffer (20 mM Tris pH 7.5, 500 mM NaCl, 10% glycerol, 0.1% Triton x-100, 1 mM benzamidine, 1 mM PMSF). The proteins were eluted with the elution buffer (30 mM reduced glutathione, 50 mM Tris-HCl pH 8.0). Purified GST-tagged proteins were run on SDS-PAGE gel and shown as bands of 73 kDa for GST-HECT or 41 kDa for GST-UBM1 (Fig 3.4).

The proteins were dialyzed to buffer (20 mM Tris pH 7.5, 500 mM NaCl) and glycerol added to a final concentration of 50% glycerol and stored in the –80ºC degree freezer.

**2.4 Biolayer Interferometry (BLI):**

Proteins (His-tagged UbVs and Ub, GST-tagged UBM and HECT) were dialyzed with the dialysis buffer (10 mM HEPES pH 7, 150 mM NaCl) and diluted to final concentrations (GST-UBM: 24 μM, GST-HECT: 18 μM , His-UbV/Ub: 100-5 μM with the assay buffer (10 mM HEPES pH 7, 150 mM NaCl, 0.005% Tween-20, 0.02 mg/ml BSA). BLI experiments were performed on Octet R4 (Sartorius) using anti-GST antibody biosensors (Cat No. 1910193) to immobilize GST-tagged HUWE1 UBM and HECT domains and using His-tagged UbV or Ub proteins as analytes. Reciprocal BLI experiments were performed on Octet R4 using anti-HIS1K biosensors (BioForte Cat No. 1910224A) to immobilize HIS-tagged UbV4 and using GST-tagged HUWE1 UBM and HECT domains as analytes. The assay buffer was used as the Ligand free control. The experiments were performed using the Octet Kinetic Module.

Sensorgram raw data was processed by Octet Analysis Studio 12 software. The equilibrium dissociation constant ($K_d$) was determined by GraphPad using sensorgram processed response (wavelength shift in nm) and analyte concentrations via the One-site specific binding equation (Eq. 1).

$$\text{Response (nm)} = B_{max}*\text{Concentration}/(K_d+\text{Concentration})$$

The data was placed in a non-linear regression model on Graphpad, which extrapolated the maximum specific binding ($B_{max}$) and $K_d$.

**2.5 Cell Growth and Treatment**

HEK 293T cells were grown in DMEM media (10% FBS, S/P antibiotics) at 37ºC, 5% $CO_2$ levels until cell confluency reached 80-90%. Media was switched every 2-3 days.

To accumulate ubiquitinated proteins in the HEK 293T cells, HEK 293T cells transfected with various UbVs were treated with 10 μM of MG132 (Cat No. 474790-5MG, EMD Millipore Corp.) for 4 hours and then harvested by trypsinization.

**2.6 Expression of mCherry-tagged or Venus-tagged UbVs in HEK 293T cells:**

The FLAG-tagged UbVs were cloned into pCDNA3.1 mCherry or Venus vectors so that the mCherry/Venus-UbV plasmids can be expressed in mammalian cells and used for probing the functions of each UbVs in mammalian cells (Table 2.2). The pET53-UbV plasmids were provided by Dr. Wei Zhang's lab (University of Guelph). The UbVs were cloned via Restriction Enzyme site cloning (Table S1). The plasmid map includes the cloning sites was shown in Figure 3.12 and Figure 3.14.

UbV PCR product of UbV was verified via agarose gel. After digestion of the PCR fragment and linearizing the fluorescent vector, the insert and vector were ligated and transformed into DH5α E. coli cells. The next day, colonies were chosen, and colonies underwent colony PCR to verify UbV insertion. Plasmids were prepared and sent for sequencing (Fig 3.12-3.15).

The cloned plasmid is transfected into HEK 293T cells using PolyJet (cat. SL100688, SignaGen. The transfection reactions containing DNA and Polyjet were summarized in Table 2.3. The efficiency of the expression was verified via fluorescence (F) (mCherry), with efficiency % ranging between 85-95%. The UbV expression level was then examined by western blot.

**Table 2.2** A table of the plasmids used for Cellular Expression

| Plasmid Name | Plasmid Type | Description |
|---|---|---|
| HU.1<br><br>(Venus-HU.1) | pcDNA3.1 Venus | An YFP-tagged plasmid. The UbV sequence was cloned with an N-terminus YFP fluorescent tag. The pcDNA 3.1-Venus plasmid was provided by the Sheng lab. |
| UbV4<br><br>(mCherry-UbV4) | pcDNA3.1 mCherry | An RFP-tagged plasmid. The UbV sequence was cloned with an N-terminus RFP fluorescent tag. The pcDNA 3.1-mCherry plasmid was provided by the Sheng lab. |
| HU.1_UbV4 fusion<br><br>(mCherry-HU.1_UbV4) | pcDNA3.1 mCherry | An RFP-tagged plasmid. The UbV sequence was cloned with an N-terminus RFP fluorescent tag. The UbVs were linked via a $(GGGGS)_2$ linkage (Chen et al., 2013). |

## 2.7 Clone and Expression of RFP (mCherry)-UbV fusion pcDNA 3.1:

HU.1 was developed for the HECT domain and UbV4was developed to bind to the UBM domain. Both HU.1 and UbV4 have been cloned and expressed in mammalian cells; a fusion protein was cloned in the mCherry plasmid and expressed in mammalian cell.

Unlike the two other clones of the fluorescent UbVs, the cloning strategy was Gibson Assembly cloning. The strategy included: (1) PCR HU.1 and UbV4 from their pET53 vectors with large segments overlapping with the linearized mCherry-pCDNA3.1. The forward primer section of UbV4 and the reverse primer section of HU.1 have an overlapping component that sequences a

flexible GGGGS repeat chain (Table S2). (2) Insert HU.1 and UbV4 PCR fragments into mCherry-pCDNA3.1 with the forward primer of HU.1 and reverse primer of UbV4 and the Gibson Assembly Master Mix (Cat. No: E2611L, New England Biolabs). (3) Transformation and colony selection using colony PCR. (4) Sequencing to verify the cloning plasmid (Fig 3.16, Table 2.1).

The fusion PCR product of HU.1_GGGGS_UbV4 (HU.1_UbV4) from both pET53-UbV vectors was verified via agarose gel (1%). An agarose gel verified the linearization of the mCherry vector linearization. After the Gibson Assembly reacted, the product was transformed into DH5α E. coli cells. Colonies grown on ampicillin-containing agar plates were then PCRed via colony PCR to verify proper insert ligation. Successful ligation was then sent to sequence three colonies at a time until proper sequencing was found (Fig 3.16).

The cloned plasmid is transfected into HEK 293T cells using PolyJet (cat. SL100688). The efficiency of the expression was first verified via fluorescences (mCherry), with efficiency % ranging between 85-95%. The UbV expression was then rechecked via expression level by western blot (1µg/µl sample concentration) (Fig 3.18B).

**2.8 Transfection of HEK 293T cells:**

The cloned plasmids were transfected into HEK 293T cells using PolyJet (cat. SL100688, SignaGen). Plasmid DNA was purified using Qiagen Maxi prep kits (Qiagen 12162). HEK 293T cells were incubated with the plasmid DNA (Table 2.3) in serum free DMEM media and diluted with PolyJet Reagent (Table 2.3) in equal volumes of serum-free DMEM media. The DNA-PolyJet mixture was incubated for 10-15 minutes to form the complex and added into the plate of cells (cell confluency: ~80%). The plate was incubated for 12-18 hours at 37ºC with 5% $CO_2$ with the DMEM media being replaced with fresh DMEM media. The cells were harvested after

transfection. The efficiency of the expression was estimated using ThermoFischer EVOS microscope with efficiency % ranging between 85-95%. The UbV expression was confirmed by western blot using Anti-Flag Antibody.

**Table 2.3:** Transfection Ratio Table:

| Plate Type | DNA | PolyJet reagent | Culture Medium | Dilution Volume |
|---|---|---|---|---|
| 6 well/35 mm | 2 ug | 3 uL | 1 mL | 2 X 0.05 mL |
| 10 cm | 7 ug | 15 uL | 5 mL | 2 X 0.25 mL |
| 15 cm | 9 ug | 20 uL | 8 mL | 2 X 0.4 mL |

## 2.9 Co-Immunoprecipitation (Co-IP):

Fluorescent-UbV proteins were expressed via transfection on a 15 cm plate. After 24-48 hours, the efficiency of the transfected cells was checked via the EVOS microscope (Thermo Fischer) (Fig 3.13B, 3.15B, 3.17B). Cells with transfected efficiency above 80% were used. The cells were trypsinized and pelleted. The pellet was washed twice with PBS and lysed with IP Lysis Buffer (25 mM Tris-HCl pH 7.4, 150 mM NaCl, 1% NP-40, 1 mM EDTA, 5% glycerol) and protease inhibitor (PI) (Cat No.1187580001, Roche, protease inhibitor cocktail tablet, cOmplete, EDTA-free). The lysate was periodically pipetted on ice for five minutes and then spun down at 13000 x g for 10 minutes at 4°C. BCA assay (Pierce BCA Protein Assay Kit, Cat No. 23225, Thermo Scientific) was conducted to determine total protein concentration. The lysate was used for Co-IP. Anti-FLAG M2 Affinity Gel (Cat No. A2220, Sigma) was pre-washed in IP lysis buffer and mixed with and 1000 µl of cell lysate. The mixture was rotated on the roller overnight. The next day, the mixture was centrifuged for 30 seconds at 5000-8200 x g, and the supernatant was removed. The resin was washed three times with TBS. The Co-IP was mixed with a Novex sample

buffer (Cat. No. LC2676, Invitrogen) 60 µl, boiled for 3 minutes, and then centrifuged for 30 seconds. The supernatant was transferred to the fresh tube for immunoblots.

**2.10 Western Blot:**

HEK 293T cells were lysed with IP Lysis Buffer (25 mM Tris-HCl pH 7.4, 150 mM NaCl, 1 mM EDTA, 1% NP-40, 5% glycerol, 1x PI, 1mM N-Ethylmaleimide (NEM) (Cat No. E3876, Sigma-Aldrich) and diluted into a 1mg/ml set of samples.

Samples were run on Novex gradient polyacrylamide gels 4-12% (Cat No. XP04120BOX, Invitrogen) and then transferred to a PVDF membrane (Cat No. 10600021, GE Healthcare) via an 18–22-hour transfer at 4$^{o}$C at 30 V. The membrane was then Ponceau S stained to verify proper transfer and blocked 2 hours with 5% milk-TBST and 1 hour 5% BSA-TBST and followed by a quick wash. The membrane was incubated with respective primary antibody (PARP1, p53 HUWE1, GAPDH, FLAG) overnight at 4$^{o}$C on the rocker (Table 2.4). After primary antibody, the membrane was washed with TBST 3 times for 5 minutes each and incubated with secondary antibody for 1 hour and 15 minutes washed four times. The membrane was incubated with ECL (Cat #: NEL105001EA, PerkinElmer) for 5 minutes and imaged using MicroChemi. After imaging the same blot was stripped and probed for GAPDH as a loading control and FLAG for transfected UbVs. PARP1, p53, GAPDH and FLAG-UbVs signals do not overlap with each other.

**Table 2.4:** Western Blot Antibodies

| Antibody | Catalogue No., Manufactor | Antibody Type | Concentrations |
|---|---|---|---|
| GAPDH | 60004-1-Ig, Proteintech | Mouse | 1:5000 |
| FLAG | F1804, Sigma | Mouse | 1:1000 |
| HUWE1 | A300-486A, Bethyl | Rabbit | 1:1000 |
| p53 (DO-1) | E2918, Santa Cruz | Mouse | 1:1000 |
| PARP1 | 14-6667-82, Invitrogen | Mouse | 1:1000 |
| Anti-Mouse-HRP | 715-035-150, Jackson Immuno | Donkey | 1:5000 |
| Anti-Rabbit-HRP | 711-035-152, Jackson Immuno | Donkey | 1:5000 |

# Chapter 3: Results

### 3.1 Protein Sequence Analysis and Structure of UbVs

Previous studies have demonstrated the versatility of UbVs as effective tools for investigating the functions of ubiquitin E3 ligases and DUBs enzymes. To create UbVs for HUWE1, phage display approach was employed for initial screening and selection using a library of ubiquitin variants. One UbV, HU.1, was selected for its specific affinity towards the HUWE1 HECT domain. Additionally, UbV4 was selected to target the first UBM domain of HUWE1 tUBM (Fig 1.7).

To further characterize these UbVs, their protein sequences were aligned and compared with Ub using Clustal Omega. 3D protein models for UbV4 and HU.1 were predicted using AlphaFold (Jumper *et al.,* 2021).

As shown in Figure 3.1 and Figure 3.2, despite HUWE1 UbVs are similar in structure and molecular size to Ub there are several structural differences. Ub is a globular protein with a typical tertiary structure comprising a 5-strand β-sheet, $3_{10}$ short helix and a central α helix (Dikic et al., 2009). However, the central β sheet of UbV4 and HU.1 only contains 4 strands. The β-sheet of Ub comprises a conserved hydrophobic patch consisting of three regions (region 1, 2, and 3), which mediates its most non-canonical interactions (Fig 3.1A) (Dikic et al., 2009). These hydrophobic regions are altered in both HUWE1 UbV models (Fig 3.2A-E). Furthermore, the C-termini of both UbV4 and HU.1 have extended tails owing to the incorporation of additional amino acids. Significantly, the C-terminal GG motif is modified so these UbVs cannot participate in ubiquitination reactions.

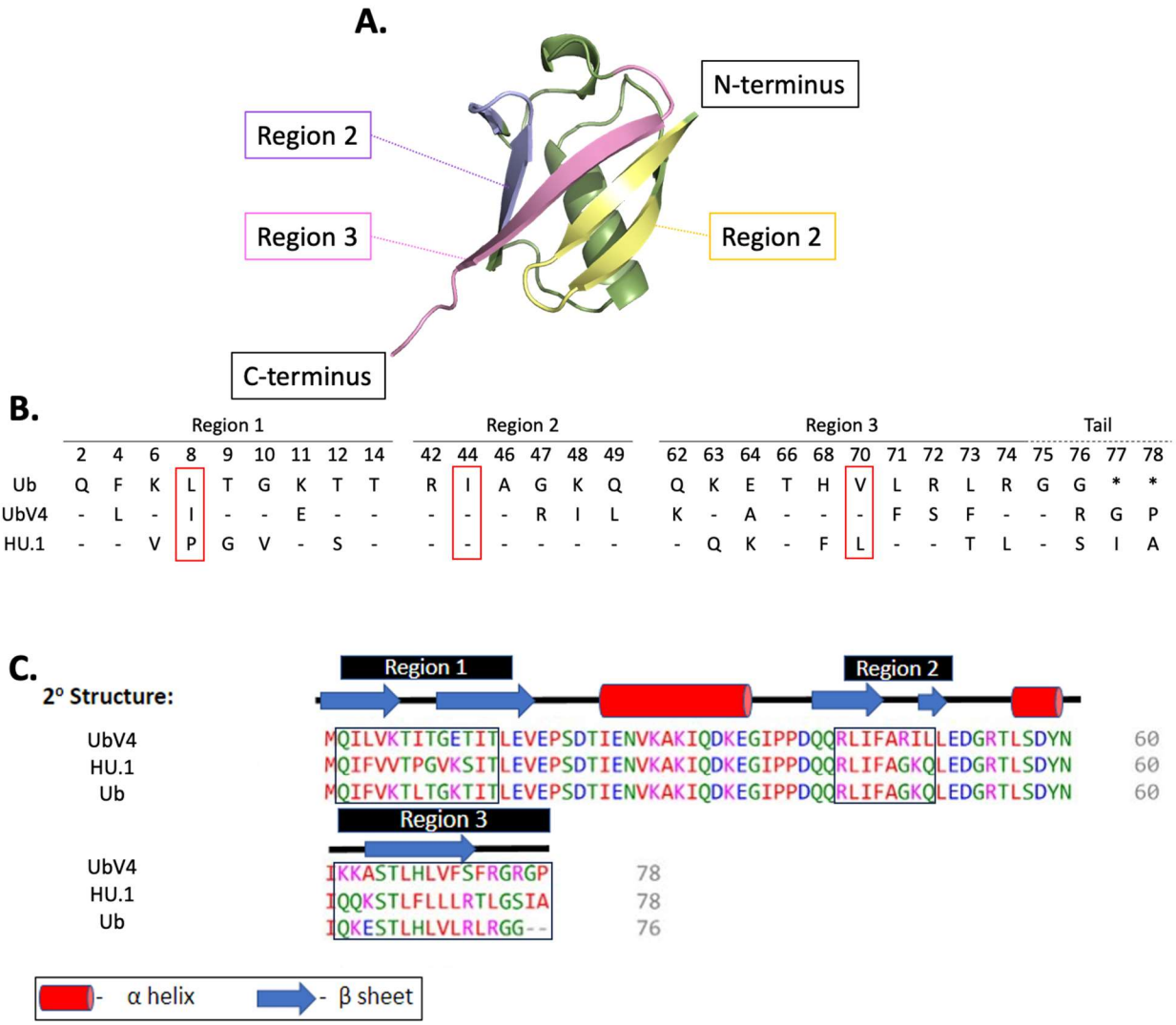


**Figure 3.1: UbV Sequence Analysis**

A) A cartoon diagram of a 3D structure of Ubiquitin (PDB: 1UBQ) highlighting the three conserved hydrophobic patch regions that are changed in UbVs. Yellow represents Region 1, purple represents Region 2, and pink represents Region 3. B) Protein amino acids sequence of the three conserved regions that compares the two UbV sequence with ubiquitin C) The sequence alignment of two HUWE1 UbVs with Ubiquitin. The Secondary structure and three conserved regions of UbV4, HU.1 and Ub are indicated.

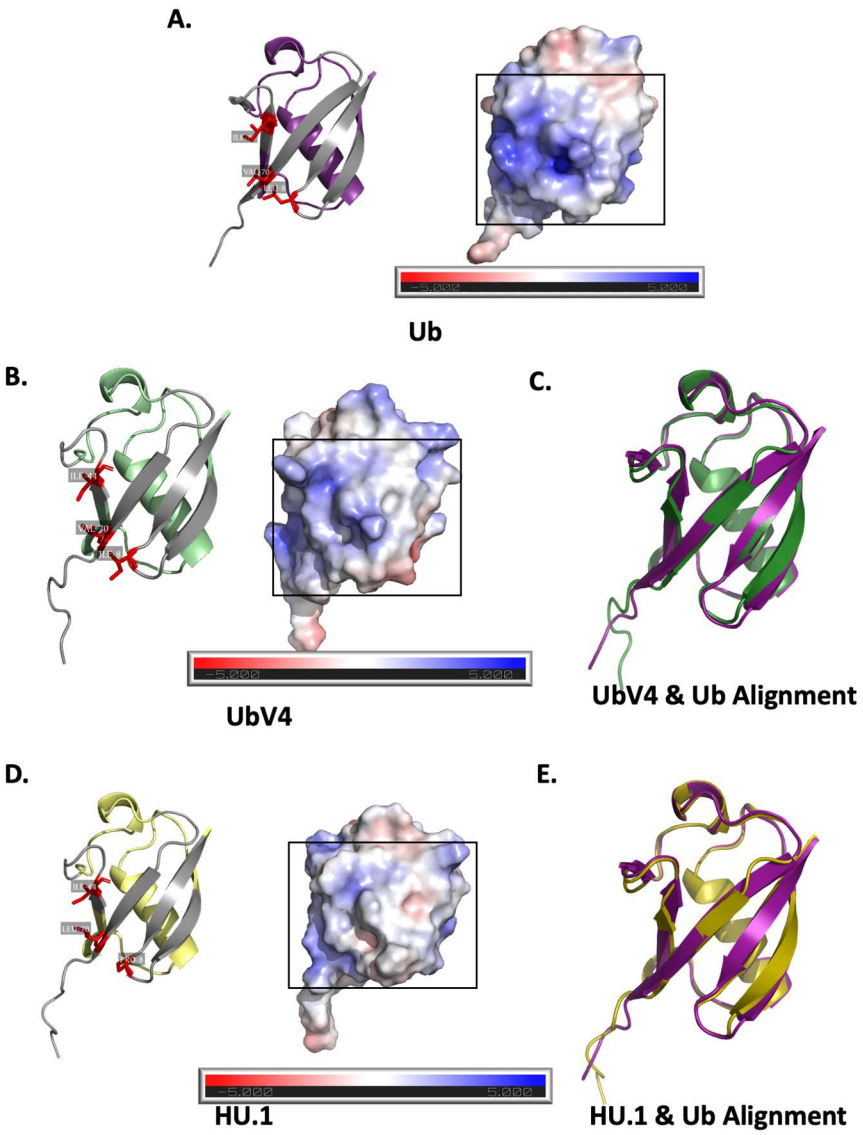


**Figure 3.2: Structural Comparison of UbV and Ub**

A) Left: 3D structure of Ub (1UBQ) depicted in a cartoon diagram (Hydrophobic patch: grey) with critical interaction residues (L8, I44, V70) indicated. Right: An electrostatic potential diagram of Ub with canonical hydrophobic patch highlighted in the box (red: negative polarity, grey: non-polar, blue: positive polarity). B) Left: 3D cartoon protein model of UbV4 made via AlphaFold (Hydrophobic patch: grey) with critical residues (I8, I44, V70) indicated. Right: An electrostatic potential diagram with canonical hydrophobic patch highlighted in the box. C) Superposition of UbV4 structural model with Ub (1UBQ). (UbV4: Green, Ub: Purple) D) Left: 3D cartoon model of HU.1 made via Alphafold (Hydrophobic patch: grey) with critical residues (P8, I44, L70) indicated. Right: An electrostatic potential diagram with canonical hydrophobic patch highlighted in the box. E) Superposition of HU.1 structural model with Ub (1UBQ) (HU.1: Yellow, Ub: Purple)). PyMol was used to prepare these diagrams.

Notably, UbV4 and HU.1 exhibit extensive mutations in three specific regions. Region 1 corresponds to Ub residues 2 to 14. This region forms the first two strands of the hydrophobic β-sheet. UbV4 contains three point mutations in region 1, including F4L, L8I, and K11E, whereas HU.1 contains five point mutations, namely K6V, L8P, T9G, G10V, and T12S (Fig 3.1B). Both UbV4 and HU.1 have point mutations on the L8 residue, which is a critical residue in Ub interactions with other proteins. Mutation of this residue might change the binding features of all non-canonical target partners.

Region 2 corresponds to Ub residues 42 to 49, forming the third and fourth strands of the β-sheet. UbV4 contains three point mutations in residues G47R, K48I, and Q49L. While HU.1 has no point mutations in region 2 (Fig 3.1B). The residue I44 was retained in both UbV4 and HU.1, which was shown to be a critical hydrophobic residue for Ub interaction.

Region 3 corresponds to the fifth strand of the β-sheet, which extends towards the C-terminus and encompasses the majority of changes in both UbVs. UbV4 contains eight point mutations, involving residues Q62K, E64A, L71F, R72S, L73F, G76R, G77, and P78. HU.1 contains nine mutations, including residues K63Q, E64K, H68F, V70L, L73T, R74L, G76S, I77, and A78 (Fig 3.1B). Similar to L8 and I44, V70 is a critical hydrophobic residue in Ub, which remains in UbV4 but mutated into a leucine residue in HU.1. Since both valine and leucine are hydrophobic amino acids, this substitution is believed to be a subtle change in the residue properties of the UbV.

In summary, although UbV4 and HU.1 retain the critical residues of Ub, the surrounding mutations of UbV4 and HU.1 in these three regions (Fig 3.1B) alter the chemical features of the protein surface increasing their hydrophobicity compared to Ub hydrophobic patch, which may enable UbVs to gain novel interactions and functions (Fig 3.2A, B, D).

### 3.2 Biochemical Characterization of UbV4 and HU.1 Interaction with HUWE1 via BLI

UbV4 and HU.1 were chosen through phage display to interact with HUWE1 UBM1 and HECT domain respectively. However, while phage display is effective in selecting UbVs bound to the target, the screening process does not yield any information about specificity or binding strength of these UbVs. To address this gap, a biochemical method known as biolayer interferometry (BLI) was used to assess the binding properties of HUWE1 with UbV4 and HU.1, thus obtaining detailed information on their interaction dynamics (Fig 3.3A).

BLI is a label-free technique for monitoring real-time protein-protein or protein-ligand interactions. BLI can be used for either quantitative or kinetic analysis. BLI uses an immobilized protein (i.e. load sample) on a biocompatible fiber-optic biosensor against the binding partner in a solution (i.e. analyte sample) (Shah & Duncan, 2014). By passing white light through the biosensor tip, BLI detects the wavelength shift when the binding partner associates with the immobilized protein, which enables the determination of the binding affinity between the load and the analyte (Fig 3.3B).

In order to perform BLI experiments examining the interaction of UbV4 and HU.1 on the HUWE1 domains. HUWE1 UBM1 and HECT domain were purified as GST-tagged fusion protein. Ub and the two UbVs including UbV4 and HU.1 were prepared as His-tagged protein (Fig 3.4).

A.

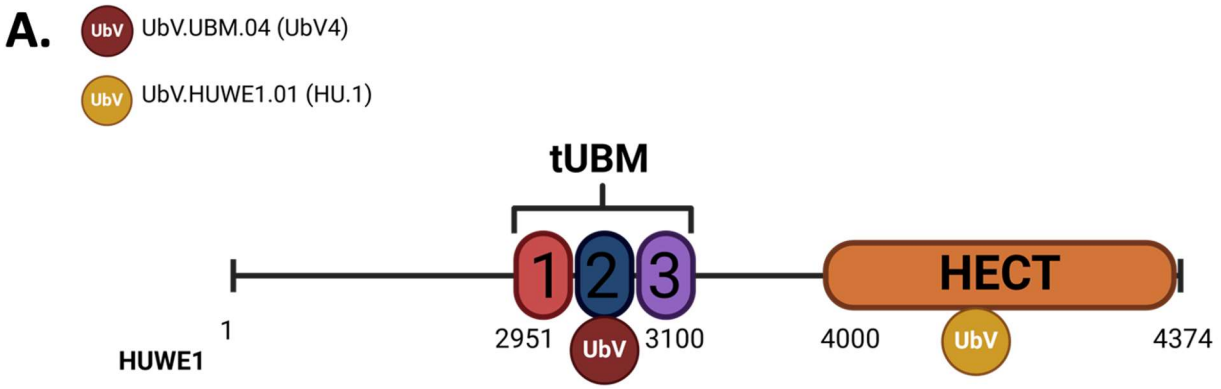


B.

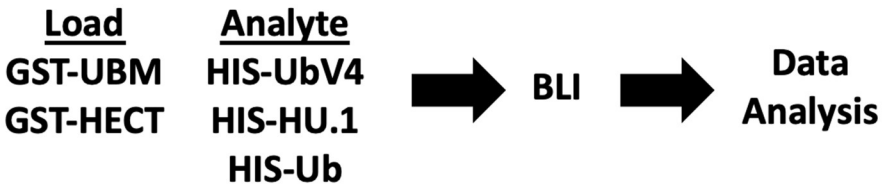


C.

| Ub/UbVs | Kd (μM) | Kd Error (μM) | $R^2$ |
|---|---|---|---|
| GST-UBM:UbV4 | 6.60 | ±1.26 | 0.98 |
| GST-HECT:UbV4 | ND | ND | 0.98 |
| GST-HECT:HU.1 | 1.43 | ±0.82 | 0.99 |
| GST-UBM:HU.1 | 20.1 | ±4 | 0.99 |
| GST-UBM:Ub | 110.6 | ± 89.34 | 0.96 |
| GST-HECT:Ub | ND | ND | 0.94 |

**Figure 3.3: Biochemical characterization of UbVs with HUWE1 using BLI**

A) A domain schematic of HUWE1, which defines the area being tested for binding Affinity via BLI B) schematic diagram showing the workflow of the biochemical characterization of UbV4 and HU.1 interaction with UBM and HECT domain C) Table of binding affinity between the UbV4, HU.1 and Ub. ND: $K_d$ not determined

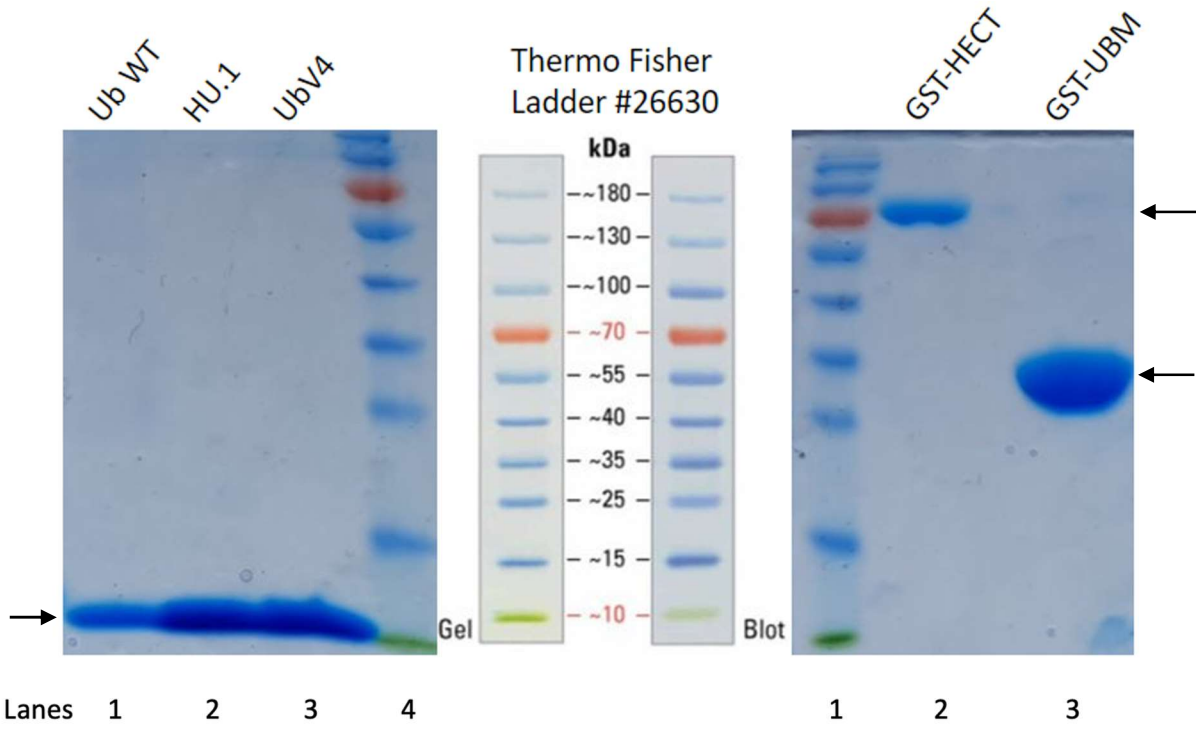


**Figure 3.4: SDS-PAGE GEL of Purified UbV/Ub and HUWE1 Domains used in BLI**

Ub, UbV4, HU.1, HUWE1 GST-HECT and HUWE1 GST-UBM proteins were purified and visualized via a 12.5% SDS-PAGE Gel using Coomassie Blue Dye. Arrows indicate the respective proteins.

### 3.2.2 Interaction of UbV4 with HUWE1 UBM and HECT domain via BLI:

Phage display has selected UbV4 specifically for targeting the HUWE1 UBM domain. To examine the interaction of UbV4 and HUWE1 UBM1, GST-tagged HUWE1 UBM was immobilized on an anti-GST biosensor as a bait protein (load sample). This bait protein was titrated using a series of increasing concentrations of UbV4 (see Fig 3.5A, B). The optical wavelength shift (nm) induced by protein-protein interaction was then translated onto a sensorgram and used in a One-site binding model equation to calculate the binding affinity between UbV4 and HUWE1 UBM (Fig 3.5). Steady-state equilibrium dissociation constant $K_d$ was calculated for the interaction.

As shown in Figure 3.5, when HUWE1 UBM was titrated with increasingly higher concentrations of UbV4, a gradual enhancement in the optical wavelength shift was observed, suggesting a correspondingly increased amount of UbV4 bound to HUWE1 UBM. Using a one-site-binding model, the steady-state $K_d$ value for UbV4 binding to HUWE1 UBM was determined to be 6.6 μM (Fig 3.3C, 3.5A, B). Since HUWE1 UBM is a Ub-binding domain, Ub was used as a control for binding to HUWE1 UBM. Ub bound to HUWE1 UBM with a steady-state $K_d$ value of 110.6 μM (Fig 3.3C, 3.6A, B ). These results confirmed that UbV4 is a binding protein for HUWE1 UBM, exhibiting a 16-fold increase in binding affinity compared to Ub.

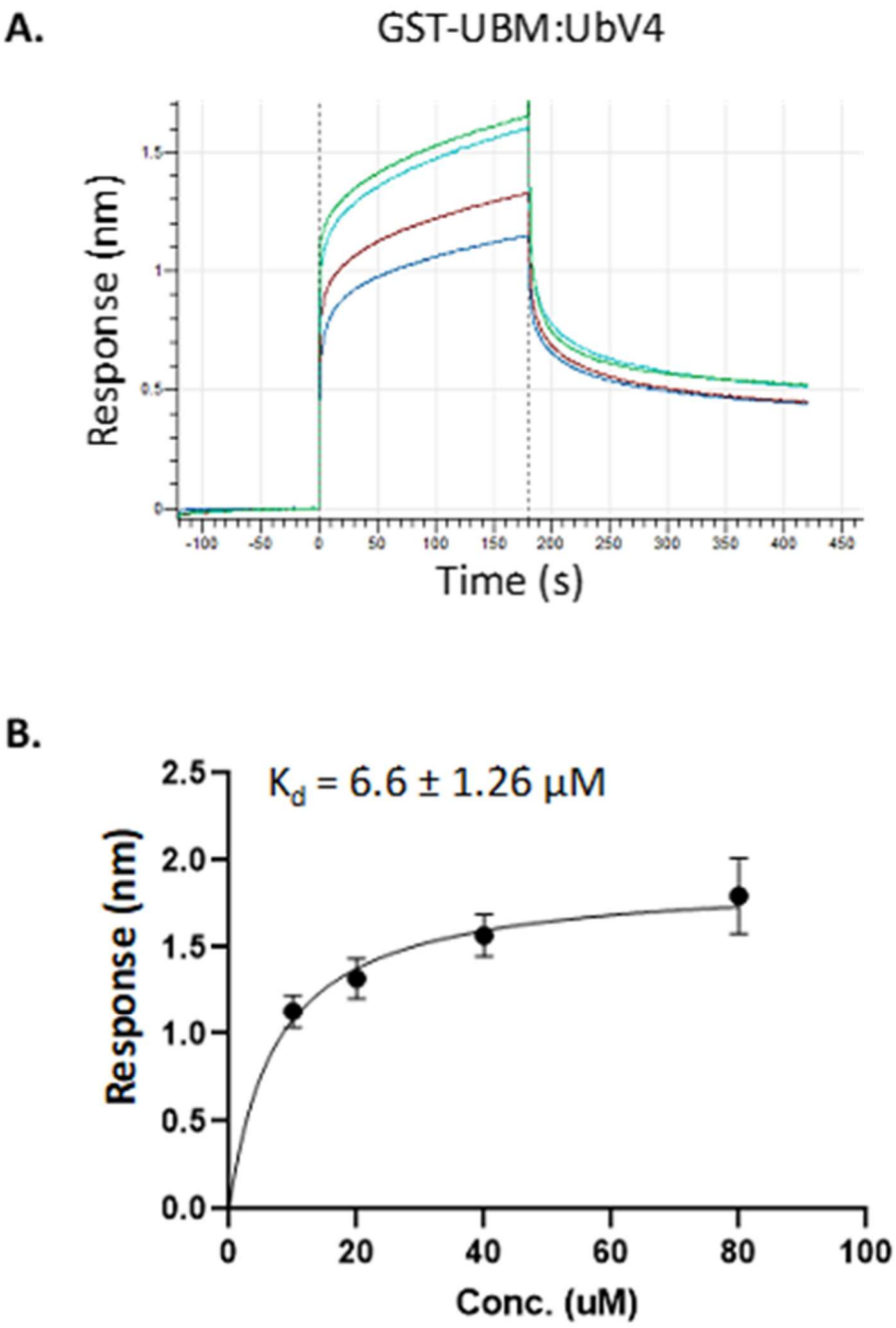


**Figure 3.5: Kinetic Analysis of UbV4 binding to HUWE1 GST-UBM domain**

A) Representative sensorgram from binding measured via BLI, with the analyte (UbV4) and an immobilized HUWE1 GST-UBM domain. B) A steady-state graph based on their interaction between the BLI data of analyte and immobilized protein interactions. Error bars show a range between three repeated tests. Concentration range (10, 20, 40, 80 µM) UbV4 and HUWE1 GST-UBM (12.5 µM).

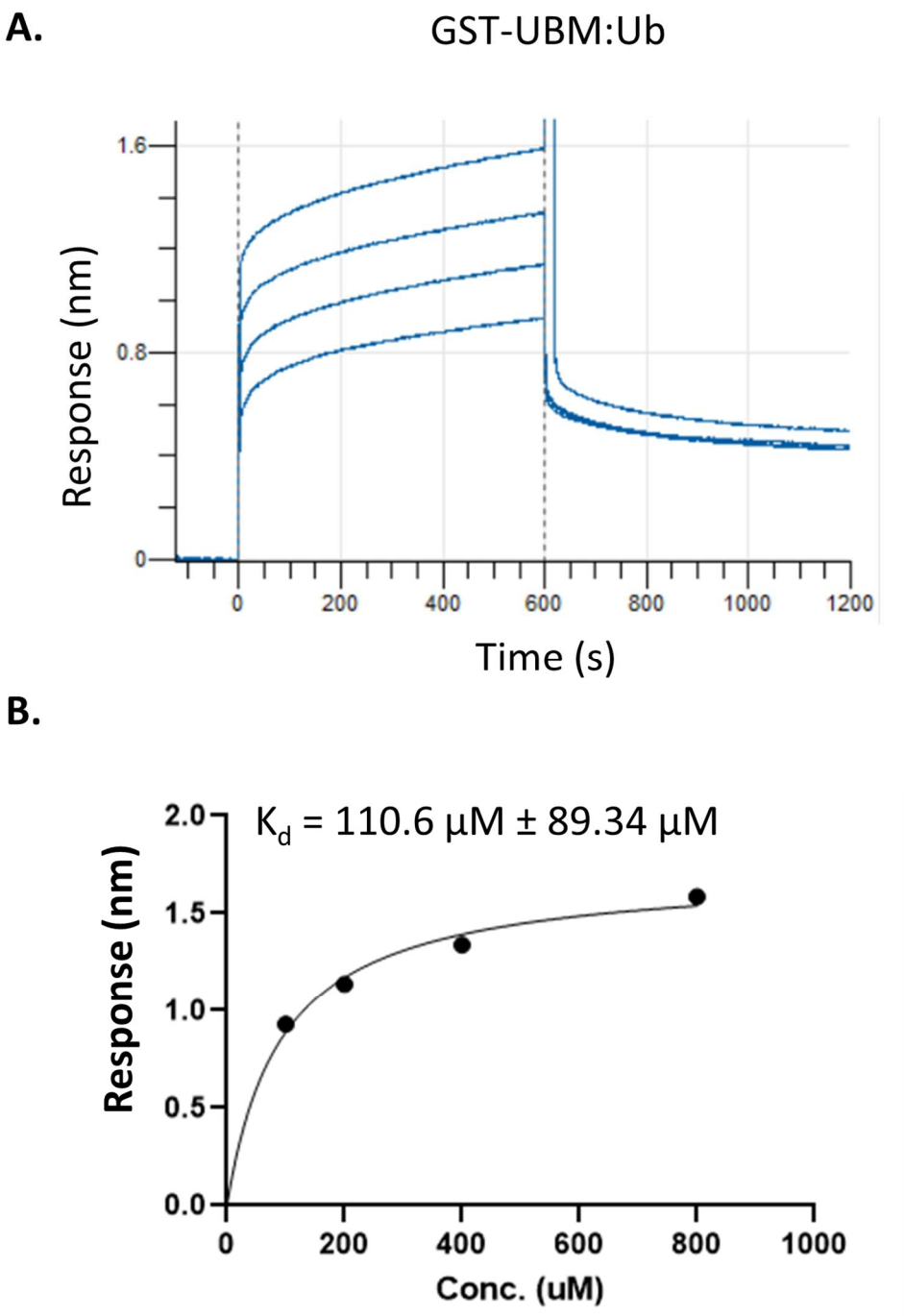


**Figure 3.6: Kinetic Analysis of Ub binding to HUWE1 GST-UBM domain**

A) Representative sensorgram from binding measured via BLI, with analyte (Ub) and an immobilized HUWE1 GST-UBM domain. B) A steady-state graph based on their interaction between the BLI data of analyte and immobilized protein interactions. Concentration range (100, 200, 400, 800 µM) Ub and HUWE1 GST-UBM (25 µM).

Many HECT domain bind Ub non-covalently to stabilize the Ub: HECT intermediate for ubiquitination (Berndsen & Wolberger, 2014). Since UbV4 structurally resembles Ub, the cross-interaction between UbV4 and the HUWE1 HECT domain was investigated. The GST-tagged HUWE1 HECT domain is immobilized on the anti-GST biosensor as bait protein, which was used to titrate with different concentrations of UbV4. Using a one-site binding model, the interaction between UbV4 and HUWE1 HECT is so weak that the steady-state $K_d$ cannot be accurately calculated (Fig 3.3C, 3.7B). This is similar to weak Ub interaction with the HUWE1 HECT domain (Fig 3.3C, 3.8B). Thus, UbV4 and Ub do not bind strongly to the HUWE1 HECT domain compared to their affinities for the HUWE1 UBM domain. These results are confirmed by a reciprocal experiment, in which the His-tagged UbV4 was immobilized and had no clear binding to the analyte, GST-tagged HUWE1 HECT domain (Fig 3.9). Together, these results demonstrated that UbV4 is a selective binder of the HUWE1 UBM domain.

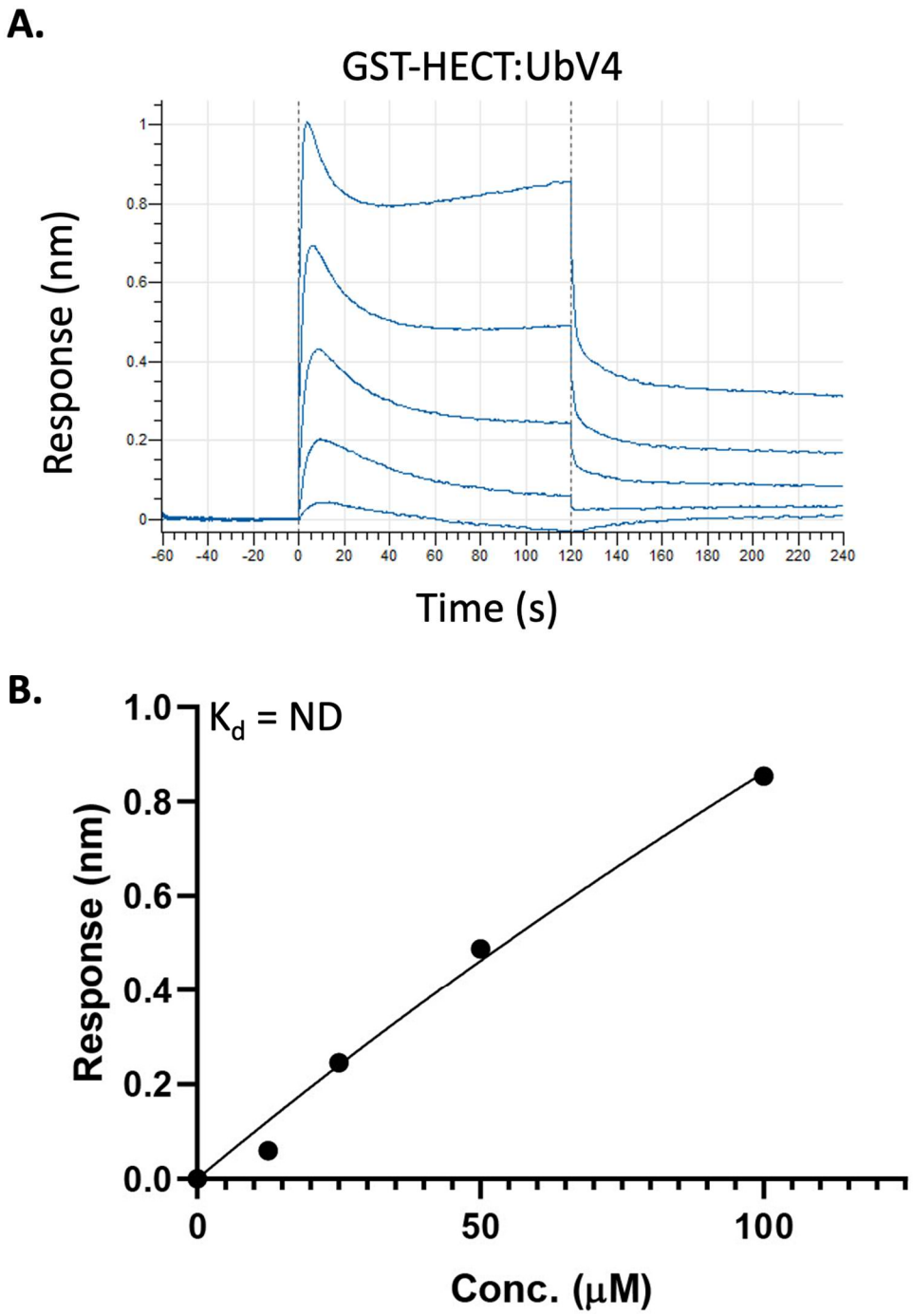


**Figure 3.7: Kinetic Analysis of UbV4 binding to HUWE1 GST-HECT domain**

A) Representative sensorgram from binding measured via BLI, with the analyte (UbV4) and an immobilized HUWE1 GST-HECT domain. B) A steady-state graph based on their interaction between the BLI data of analyte and immobilized protein interactions. Error bars are not shown due to repeats being conducted via immobilized His-UbV4. Concentration range (12.5, 25, 50, 100 μM) UbV4 and HUWE1 GST-HECT (18 μM). ND: $K_d$ not determined

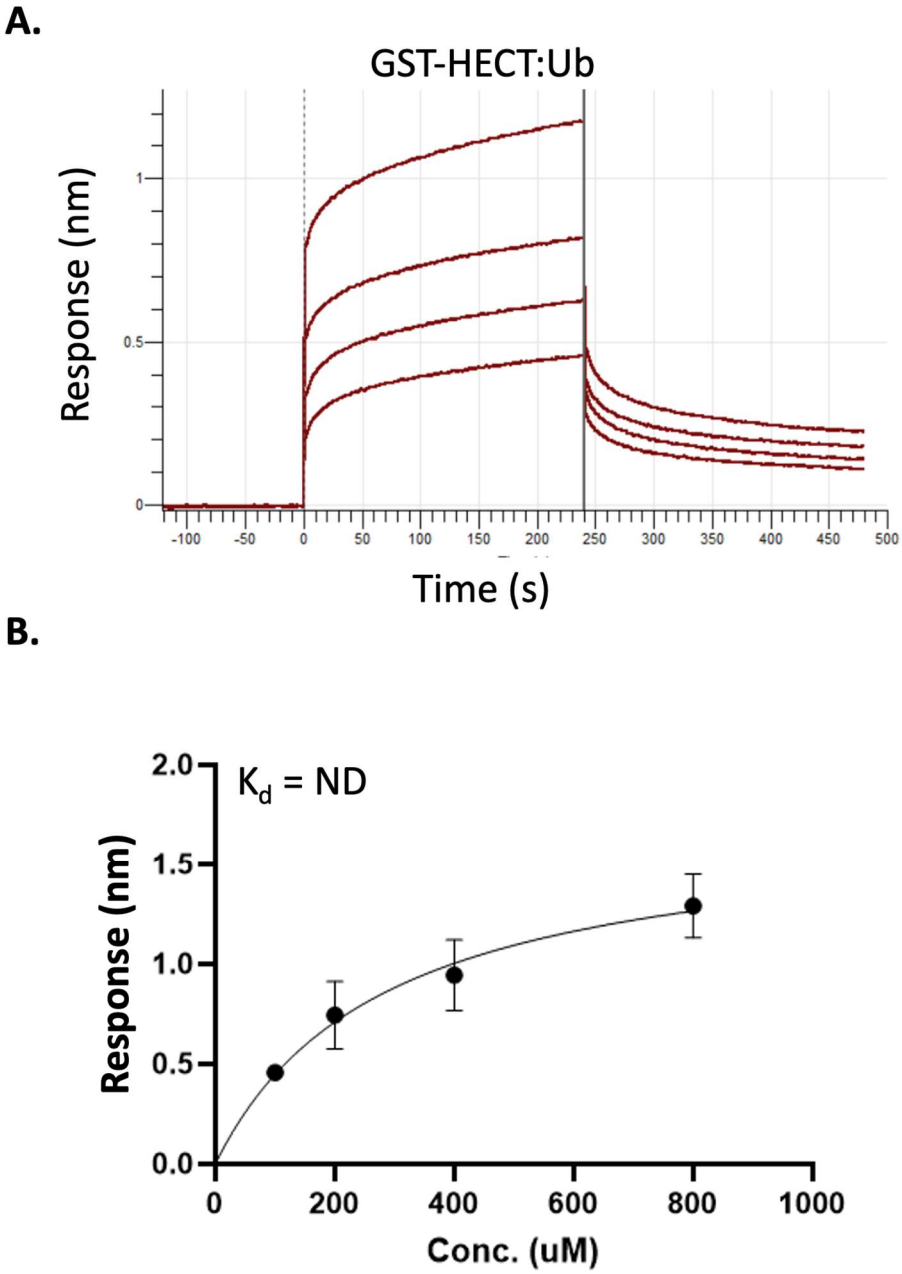


**Figure 3.8: Kinetic Analysis of Ub binding to HUWE1 GST-HECT domain**

A) Representative sensorgram from binding measured via BLI, with analyte (Ub) and an immobilized HUWE1 GST-HECT domain. B) A steady-state graph based on their interaction between the BLI data of analyte and immobilized protein interactions. Error bars show SEM between three repeated tests. Concentration range (100, 200, 400, 800 µM) Ub and HUWE1 GST-HECT (12.5 µM). ND: $K_d$ not determined

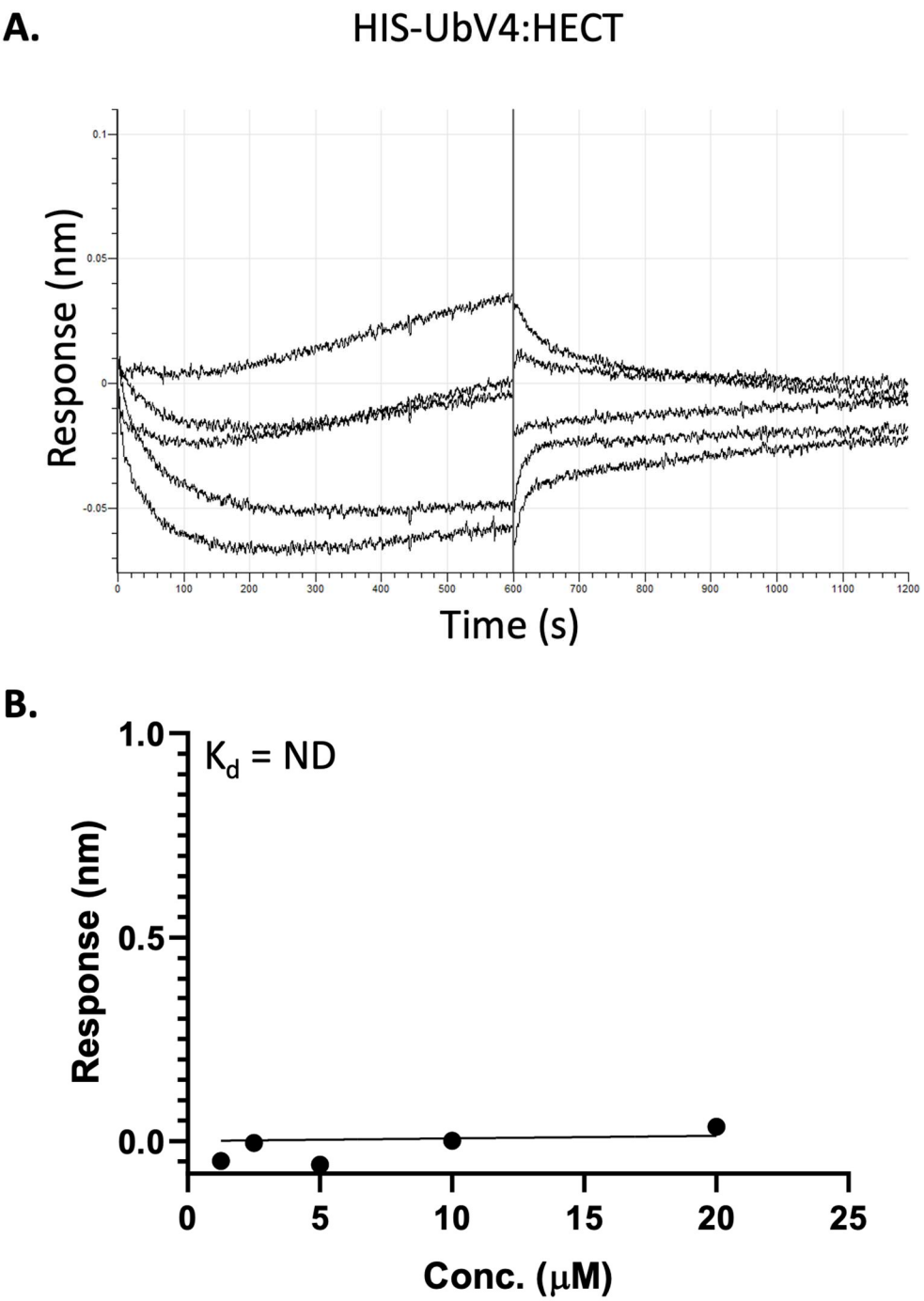


**Figure 3.9: Kinetic Analysis of HUWE1 HECT domain binding to HIS-UbV4**

A) Representative sensorgram from binding measured via BLI, with the analyte (HUWE1 GST- HECT) and an immobilized HIS-UbV4. B) A steady-state graph based on the interaction between the BLI data of analyte (HUWE1 GST- HECT) and immobilized protein (HIS-UbV4) interactions. Concentration range (1.25, 2.5, 5, 10, 20 μM) HUWE1 GST-HECT and HIS-UbV4 (100 μM). ND: $K_d$ not determined

### 3.2.2 Interaction of HU.1 with HUWE1 HECT and UBM domain via BLI:

Another UbV, HU.1, has been selected by phage display to bind to the HUWE1 HECT domain. A previous study demonstrated that HU.1 is specifically bound to the HUWE1 HECT domain and showed no affinity for other HECT domain proteins via an ELISA Assay (Zhang *et al.,* 2016). To characterize the HU.1 interaction with the HUWE1 HECT domain using BLI, GST-tagged HUWE1 HECT was immobilized on a GST sensor and titrated with different concentrations of HU.1. Consistent with the previous report; the results showed that HU.1 bound strongly to the HUWE1 HECT domain with a steady-state $K_d$ value of 1.17 μM (Fig 3.3C, 3.10A, B). Compared to UbV4 and Ub, HU.1 has the strongest binding affinity to the HUWE1 HECT domain (Fig 3.3C, 7B, 8B, 10B).

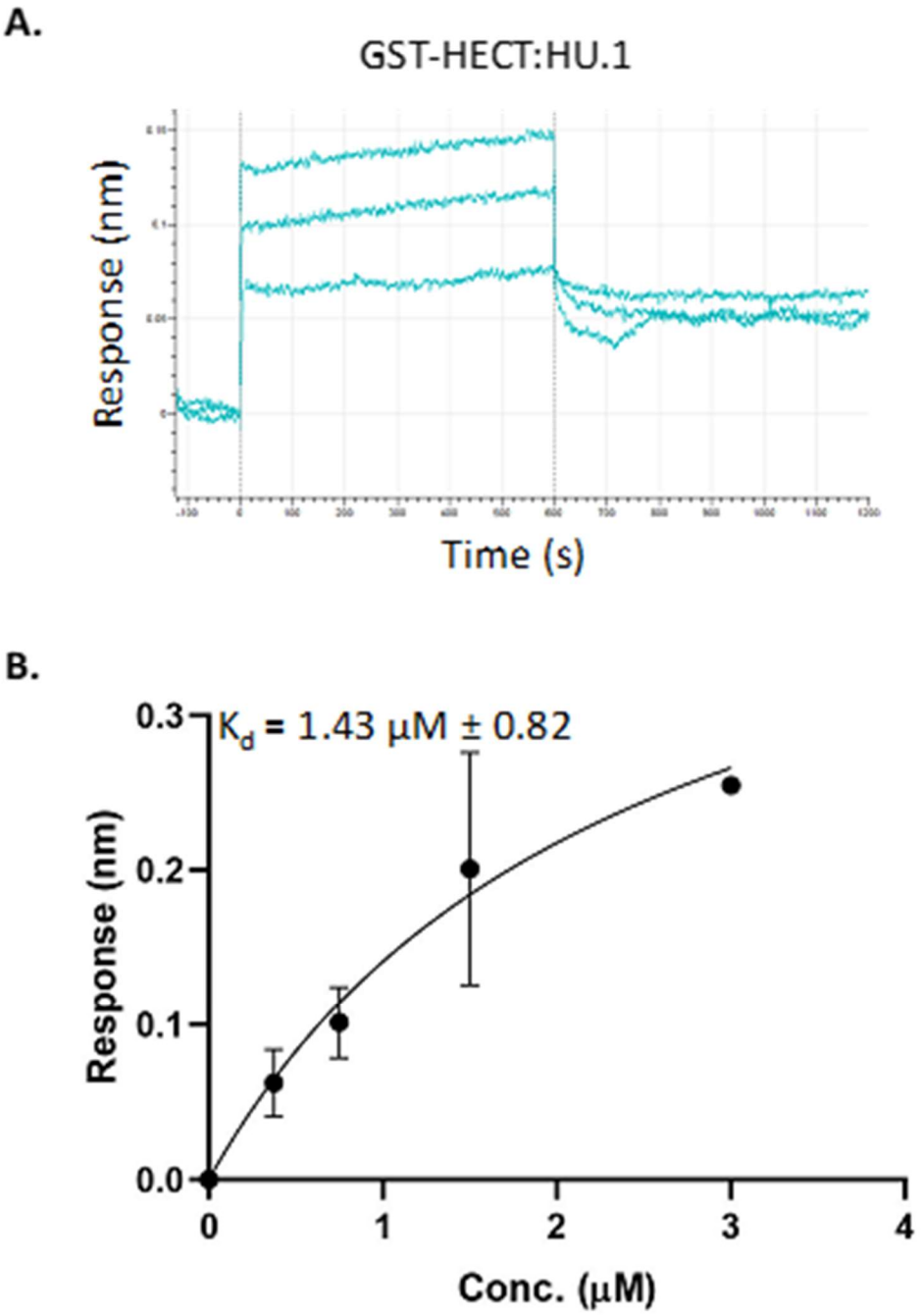


**Figure 3.10: Kinetic Analysis of HU.1 binding to HUWE1 GST-HECT domain**

A) Representative sensorgram from binding measured via BLI, with the analyte (HU.1) and an immobilized HUWE1 GST-HECT domain. B) A steady-state graph based on the interaction between the BLI data of analyte (HU.1) and immobilized protein (HUWE1 GST-HECT) interactions. Concentration range (3.75, 7.5, 15 µM) HU.1 and HUWE1 GST-HECT (12.5 µM).

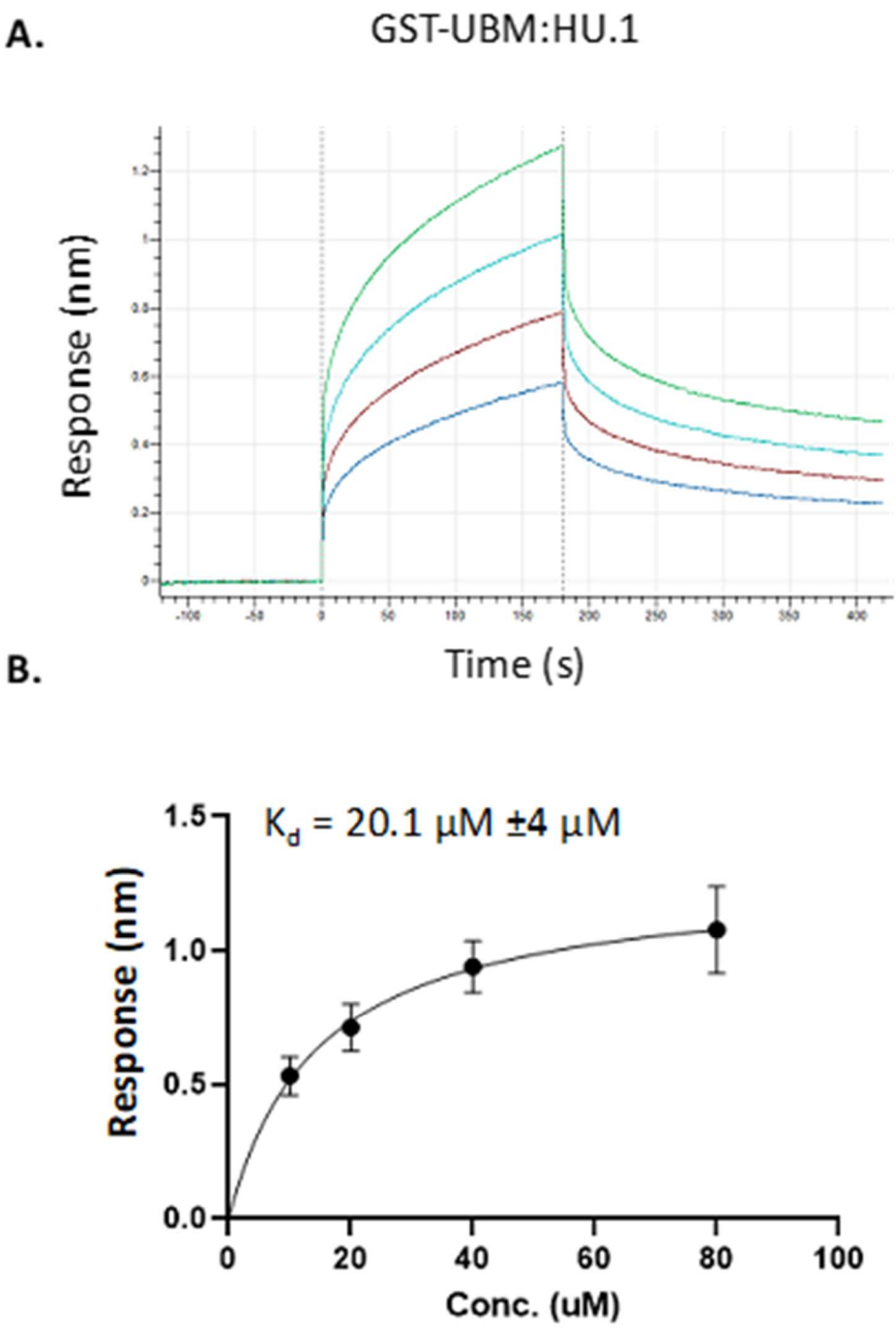


**Figure 3.11: Kinetic Analysis of HU.1 binding to HUWE1 GST-UBM domain**

A) Representative sensorgram from binding measured via BLI, with the analyte (HU.1) and an immobilized HUWE1 GST-UBM domain. B) A steady-state graph based on their interaction between the BLI data of analyte and immobilized protein interactions. Error bars show the SEM between three repeated tests. Concentration range (10, 20, 40, 80 µM) HU.1 and HUWE1 GST-UBM (25 µM).

HU.1 has a similar structure to Ub. Since the UBM domain is a Ub-binding domain, it is interesting to examine whether the HUWE1 UBM domain could also recognize HU.1. To test HU.1 interaction with HUWE1 UBM domain, GST-tagged HUWE1 UBM was immobilized on an anti-GST biosensor as a bait protein, and then titrated with increasing concentrations of HU.1. The results showed that HU.1 bound to the HUWE1 UBM domain with a steady-state $K_d$ value of 20.1 μM (Fig 3.3C, 3.11A, B). It suggests that the HUWE1 UBM domain can recognize HU.1. The affinity of HU.1 for HUWE1 UBM is weaker than UbV4 ($K_d$ = 6.6 μM) but more potent than Ub ($K_d$ = 110.6 μM) (Fig 3.3C, 3.5B, 3.6B). This study validates HU.1 as a strong HECT domain binder, but it also cross-reacts with the HUWE1 UBM domain.

### 3.3 Investigation of the cellular interactions between UbVs and HUWE1

The BLI experiments showed that both UbV4 and HU.1 bind to their selective domain of HUWE1. However, BLI is a biochemical technique; the BLI data does not prove that the UbV binds to HUWE1 in the cell. To further validate these findings, the cellular interactions of UbV4 and HU.1 with HUWE1 are examined via co-immunoprecipitation (Co-IP). Co-IP is a method used to identify protein-protein interaction in a cell, in which antibodies are employed to pull down specific proteins along with the interacting proteins.

#### 3.3.1 Interaction of mCherry-UbV4 with endogenous HUWE1 in HEK 293T cells

First, FLAG-tagged UbV4 was cloned into a mammalian pCDNA 3.1-mCherry vector (mCherry). The plasmid containing FLAG-tagged UbV4 was confirmed by sequencing (Fig 3.12). Then, the mCherry FLAG-tagged UbV4 was transfected into the HEK 293T cells (Fig 3.13A). The plasmid expression was confirmed through fluorescent microscopy (Fig 3.13B). To examine the interaction between UbV4 and HUWE1 in HEK 293T cells, Anti-FLAG-M2 beads were used for

immunoprecipitation of FLAG-tagged mCherry-UbV4. The immunoprecipitant was subjected to western blot, and FLAG and HUWE1 antibodies were used to detect FLAG-tagged mCherry-UbV4 and endogenous HUWE1, respectively. As shown in Figure 3.13C, the FLAG-M2 antibody pulled down FLAG-tagged mCherry-UbV4 together with endogenous HUWE1 (lane 1). As a Co-IP negative control, an empty pCDNA 3.1 mCherry (RFP) was expressed in HEK 293T cells and did not pull down endogenous HUWE1. These results confirm that UbV4 binds with HUWE1 in the cell. One noticeable caveat is that the mCherry-UbV4 Western Blot showed two bands, one corresponding to the correct size of FLAG-tagged mCherry-UbV4 (~36 Kda) and another at the size of FLAG-tagged mCherry (~26Kda) that might have resulted from a partial proteolysis between UbV4 and mCherry (Fig 3.13C).

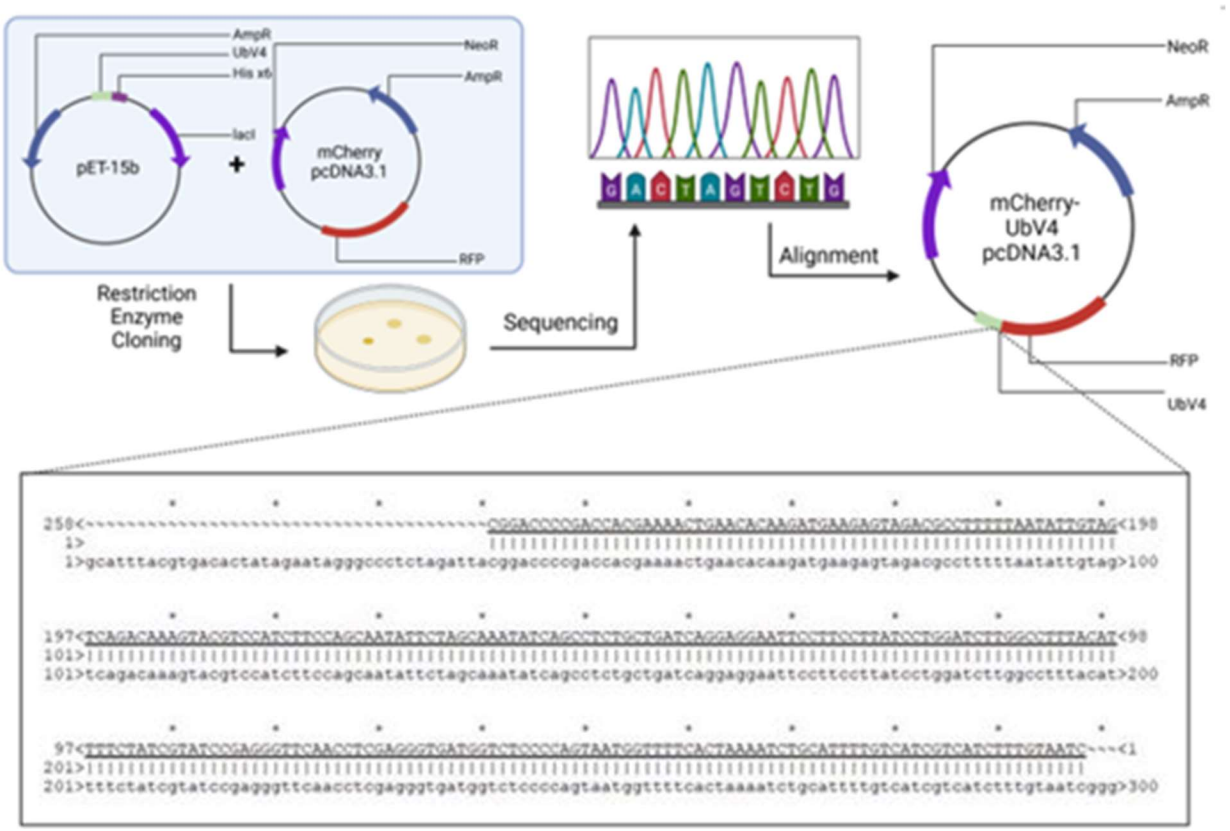


**Figure 3.12: Restriction Enzyme Cloning Flowchart for UbV4**

A flowchart of the UbV4 Cloning Process (Created by BioRender). UbV UbV4 was cloned via Restriction Enzyme Cloning. RE sites BamHI and XbaI were used for the insertion of the UbV4 insert. The Cloned plasmid E. coli was spread on plates sequences and cross-referenced to verify complete cloning.

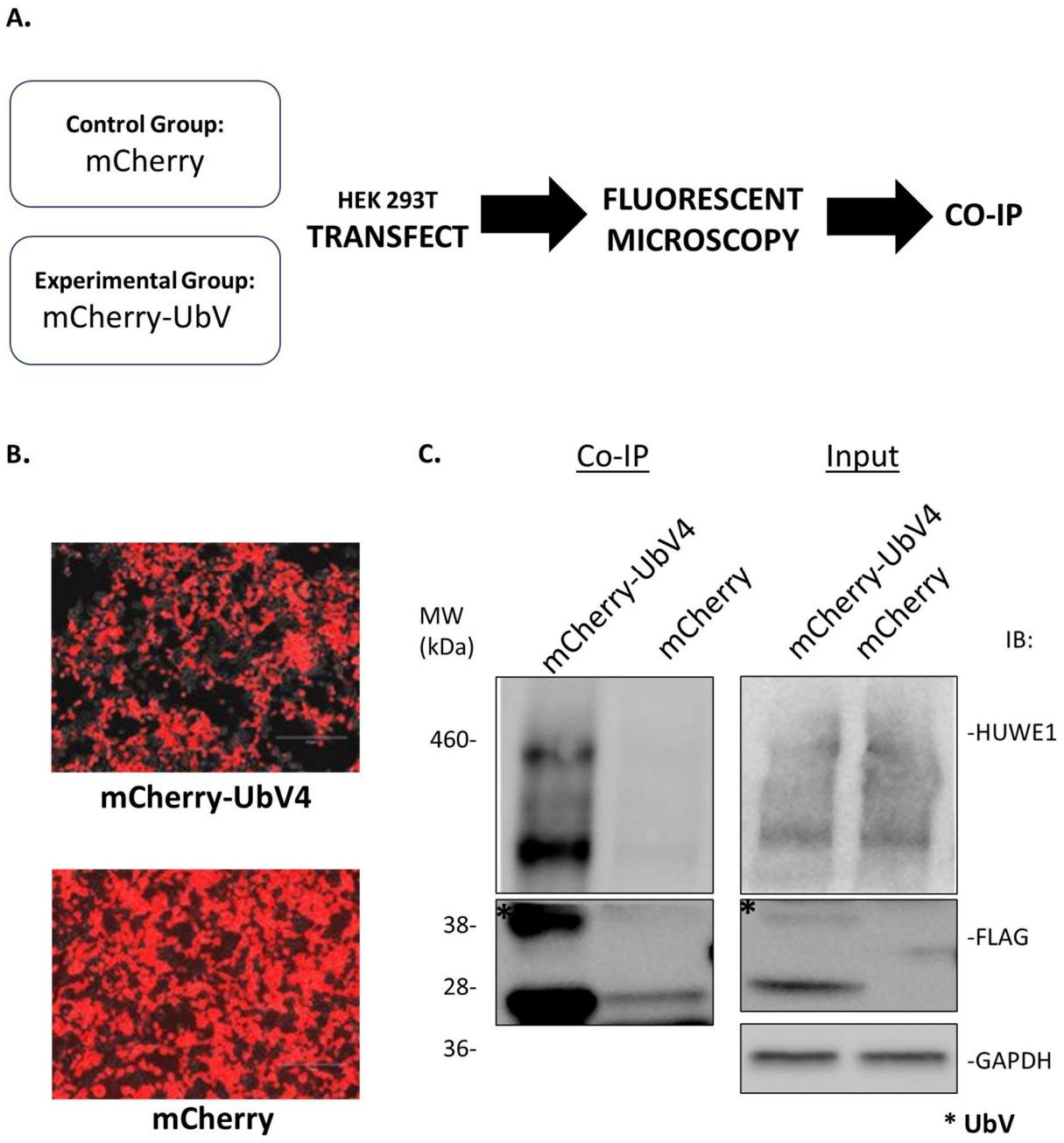


**Figure 3.13: Characterization of interaction between mCherry-UbV4 and HUWE1 using Co-IP**

A) Experimental Design of the Co-Immunoprecipitation B) The Trans, RFP image of the mCherry-UbV4 and mCherry 15 cm plate. Transfection efficiency ranged between 85-95% C) Western blot of the Co-IP of mCherry-UbV4 and mCherry (empty vector). The HUWE1 and Flag proteins were blotted. GAPDH was used as a control in the input sample.

### 3.3.2 Interaction of Venus-HU.1 with endogenous HUWE1 in HEK 293T cells

The characterization of the interaction between HU.1 and cellular HUWE1 was similar to what was described for UbV4. Flagged-tagged HU.1 was cloned into a pCDNA 3.1. YFP (Venus) vector and confirmed by sequencing (Fig 3.14). The plasmid was transfected in HEK 293T cells and its expression was verified through fluorescent microscopy (Fig 3.15B). Next, IP was performed on HEK 293T cells overexpressed with Flagged-tagged HU.1. The immunoprecipitant was pulled down with Anti-FLAG-M2 beads and further examined with western blot using Anti-FLAG and Anti-HUWE1 antibodies. The results showed that the Anti-FLAG-M2 beads was able to pull down FLAG-tagged Venus-HU.1 along with the endogenous HUWE1, demonstrating that HU.1 can interact with HUWE1 in the cell (Fig 3.15C).

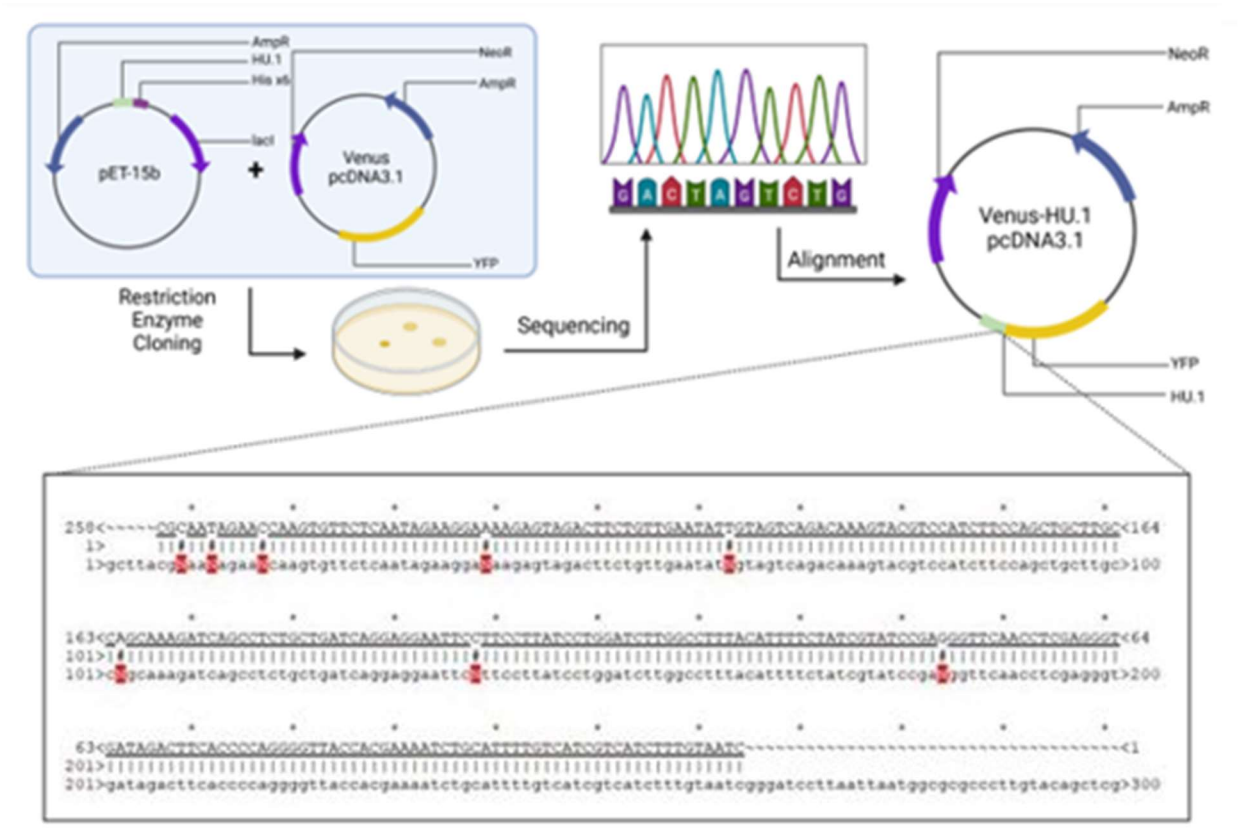


**Figure 3.14: Restriction Enzyme Cloning Flowchart for HU.1**

Diagram of HU.1 Cloning Process (Created by BioRender). UbV HU.1 was cloned via Restriction Enzyme (RE) Cloning. RE sites BamHI and NotI were used for the insertion of the HU.1 insert. The Cloned plasmid E. coli was spread on plates sequences and cross-referenced to verify complete cloning. Any red markers on sequencing were cross referenced with the Chromatography data of the sequencing data.

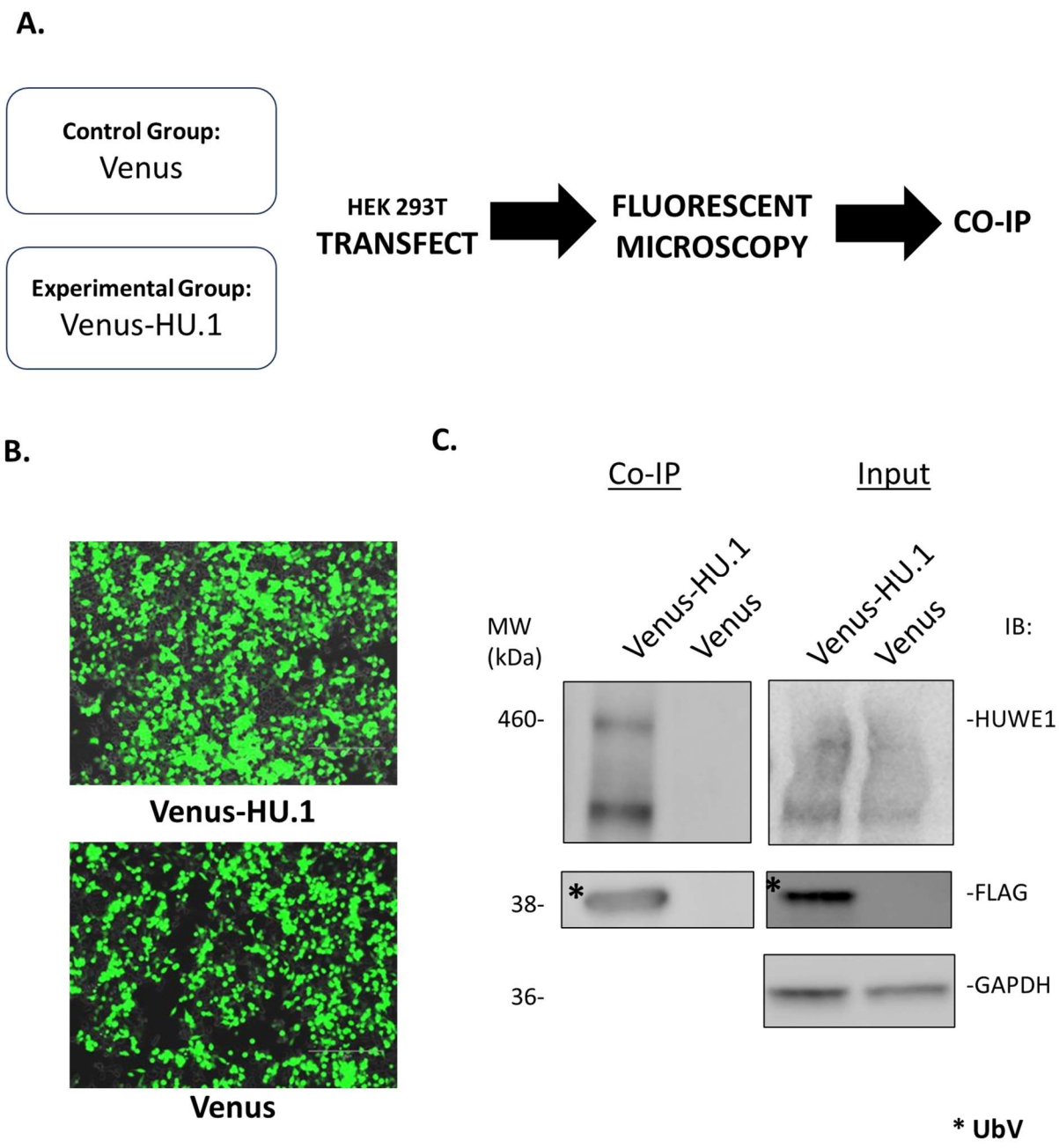


**Figure 3.15: Characterization of interaction between Venus-HU.1 and HUWE1 using Co-IP**

A) Experimental Design of the Co-Immunoprecipitation B) YFP signal of the Venus-HU.1 and Venus transfected HEK 293T cells. Transfection efficiency ranged between 90-95% C) Western blot of the Co-IP of Venus-HU.1 and Venus (Empty vector). The HUWE1 and Flag proteins were blotted. GAPDH was used as a control in the input sample.

### 3.3.3 Generation of a dual UbV (mCherry-HU.1-UbV4) and its Interaction with HUWE1

Since HU.1 binds to the HUWE1 HECT domain, and UbV4 targets HUWE1 UBM, it would be interesting to test whether a dual UbV could be a better probe for HUWE1. To create a dual UbV, HU.1 and UbV4 were fused via a ten-residue flexible link known as a GS linker ($(GGGGS_2)$) based on a previous publication (Chen et al., 2013) and cloned in a pCDNA3.1-mCherry vector using a Gibson Cloning approach (Gibson, 2011). Within the link, the eight glycines provide flexibility, and the two polar serines provide solubility (Chen et al., 2013). The plasmid was verified via sequencing, as shown in Figure 3.16. Following transfection into HEK 293T cells, the dual UbV expression was confirmed through fluorescent microscopy and western blot (Fig 3.17B, C).

Next, the FLAG-tagged mCherry-HU.1_GGGGS_UbV4 (HU.1_UbV4) fusion was subject to Co-IP to examine its interaction with HUWE1. The mCherry vector served as a negative control. The results showed that the Co-IP using FLAG antibody M2 beads pulled down the dual UbV and endogenous HUWE1. This demonstrates that the dual UbV, HU.1_UbV4 protein, binds to endogenous HUWE1 (Fig 3.17C).

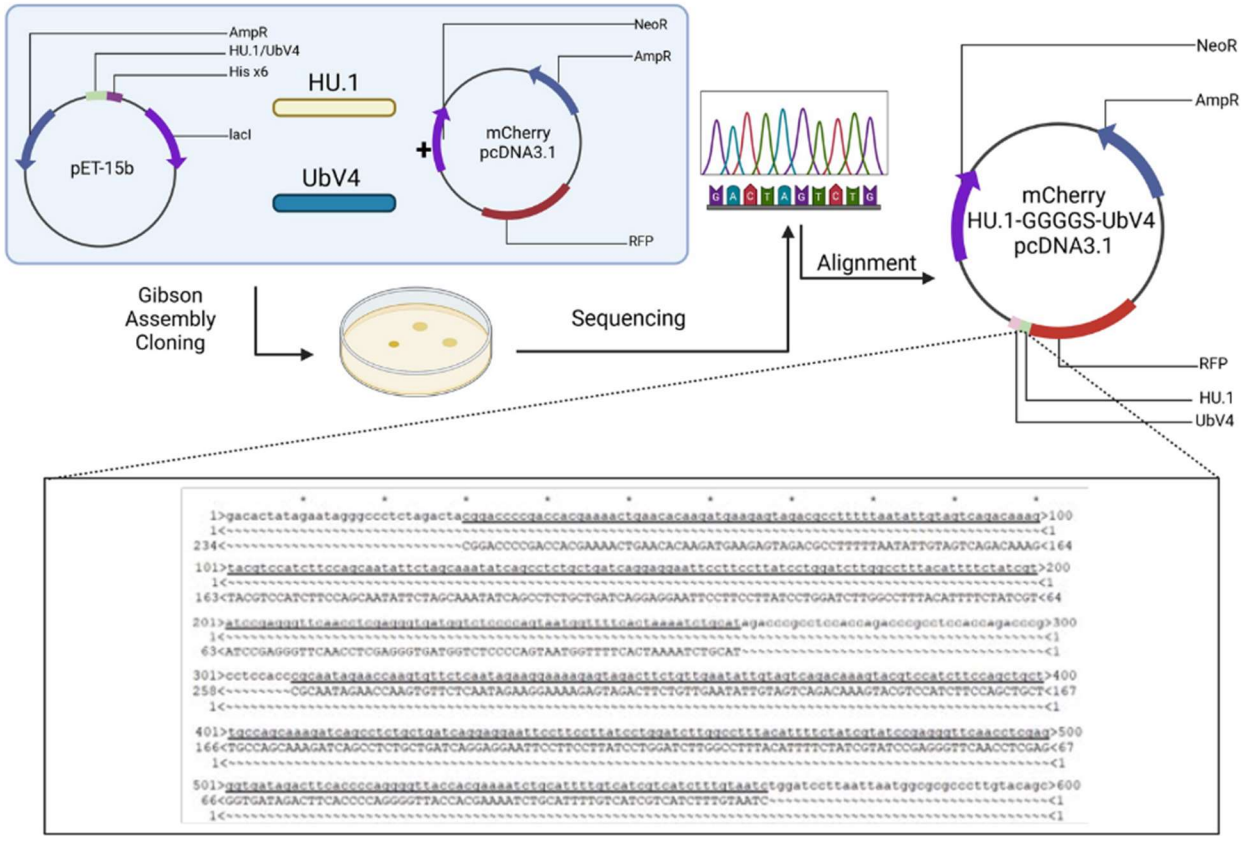


**Figure 3.16: Gibson Cloning Flowchart for HU.1-GGGGS-UbV4**

Diagram of HU.1-GGGGS-UbV4 fusion Cloning Process (Created by BioRender). UbV HU.1 and UbV4 were fused with a GGGGS linker through Gibson Assembly cloning. The Cloning were spread on plates sequences and cross-referenced to verify complete cloning (Gibson, 2011)

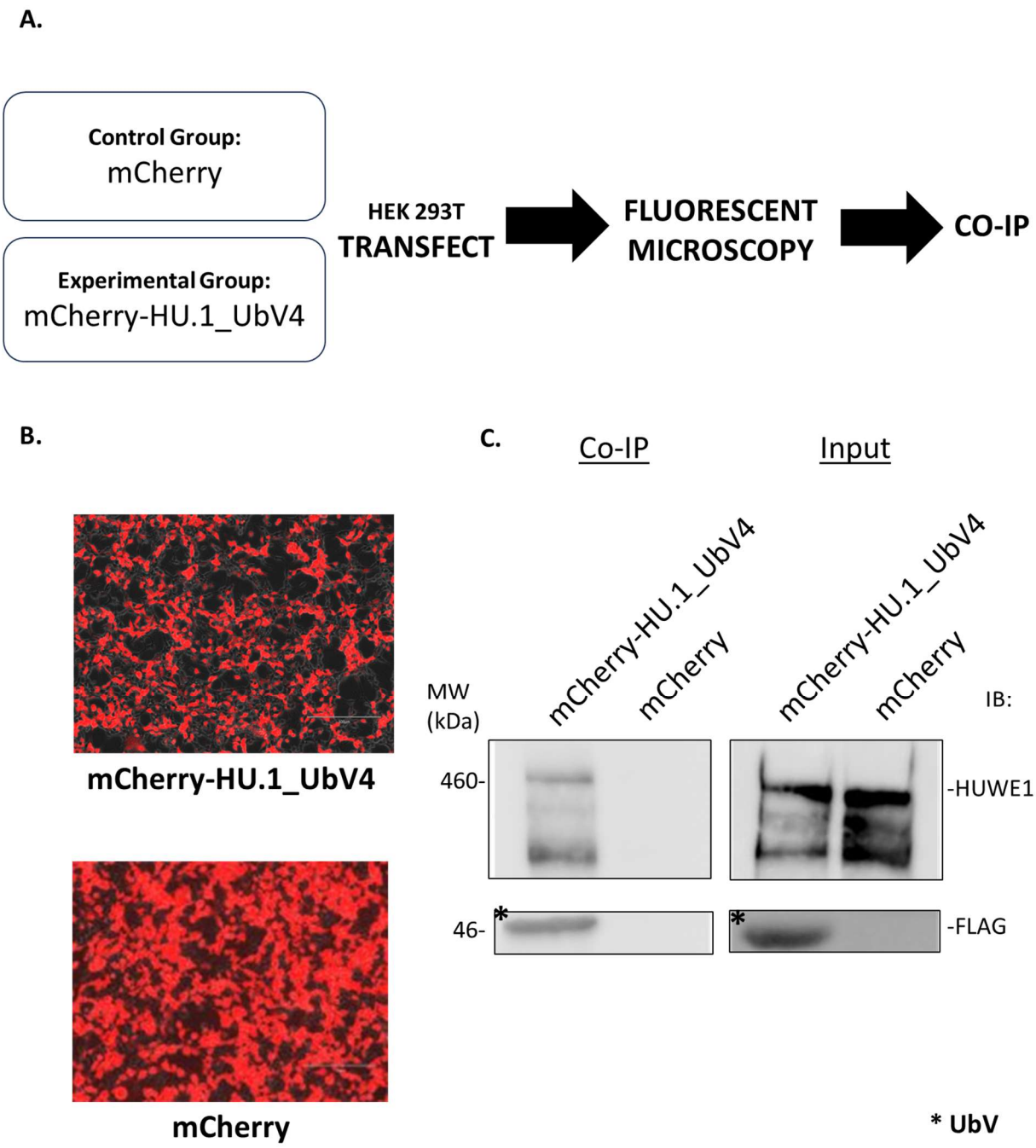


**Figure 3.17: Characterization of interaction between mCherry-HU.1_UbV4 and HUWE1 using Co-IP**

A) Experimental Design of the Co-Immunoprecipitation B) The Trans and RFP image of the mCherry-HU.1_UbV4 and mCherry 15 cm plate. Transfection efficiency ranged between 85-95% C) Western blot of the Co-IP of mCherry-HU.1_UbV4 and mCherry (Empty vector). The HUWE1 and Flag proteins were blotted.

### 3.4 Investigation of the modulatory effect of UbVs on HUWE1:

HU.1 and UbV4 have been shown to interact with HUWE1 biochemically through BLI and in cells via Co-IP. Previous research on UbV showed that UbVs may have modulatory effects on HECT domain activities and functions. Depending on where UbV interacts with the HECT domain, UbV can work either as an inhibitor or an activator of the target HECT E3 ligase. Since HUWE1 is a HECT domain E3 ligase, the modulatory effect of its UbV on HUWE1 ubiquitination and its substrates was investigated (Fig 3.18A, B).

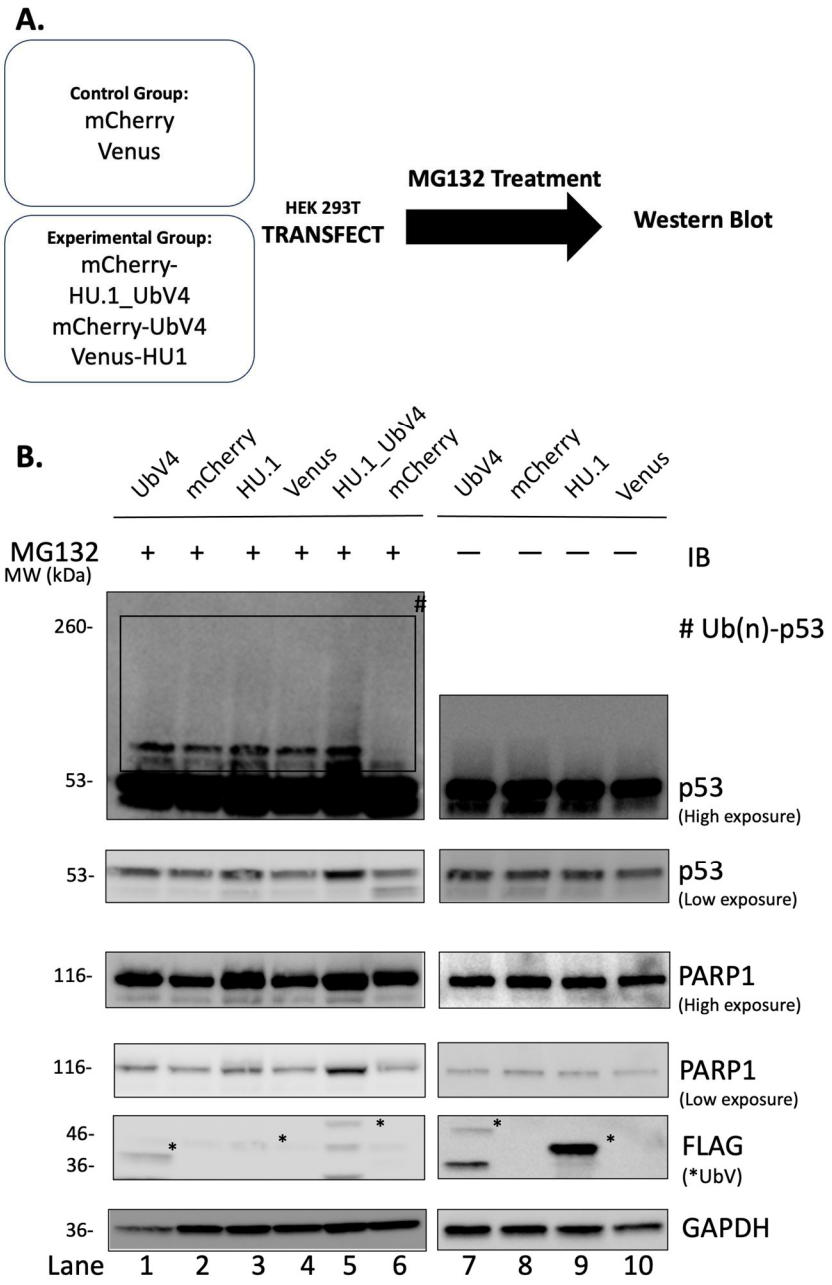


**Figure 3.18: Investigation of modulatory effects of UbVs on HUWE1 substrates**

A) A schematic of an exploratory assay of ubiquitination in cells. Plasmids are transfected into HEK 293T cells and treated with MG132 to maintain ubiquitination. The proteins were then visualized via western blot. B) Western blot of HU.1, UbV4, and dual UbV testing p53 and Ub(n)-p53 (indicated in the boxed) for modulation of ubiquitination. These are compared against untreated cell lysates of HU.1 and UbV4 via high exposure and low exposure. PARP1 showed increased levels in MG132 treated cells, while there was a decrease in untreated cells.

When a protein is ubiquitinated, one or more ubiquitin molecules are covalently conjugated to the protein, which can be visualized as a ladder or smear above the protein in a Western blot. Since both UbVs bind to HUWE1, the potential changes in HUWE1 activity can be detected by changes in levels of polyubiquitinated substrates. A previous lab member, Wen Yi, conducted a biochemical ubiquitination assay to examine the modulatory effect of UbV4 on HUWE1 HECT-mediated ubiquitination (http://hdl.handle.net/10315/39614). In this assay, she reconstituted ubiquitination reactions by providing recombinant activating enzyme E1, conjugating enzyme UbE2L6, and used the fusion of HUWE1 tUBM-HECT domain as the E3. The results show a low amount of UbV4 stimulated HUWE1 tUBM-HECT domain activity, whereas a high level of UbV4 inhibited HUWE1 tUBM-HECT domain activity. It suggests that UbV4 has both stimulatory and mild inhibitory effects on HUWE1-mediated polyubiquitination depending on the stoichiometric ratio of UbV4 relative to the HUWE1 tUBM-HECT domain.

In this study, MG132 treatment was used to investigate the modulatory effects of UbV on HUWE1 activity in HEK 293T cells. The chemical compound MG132, a proteasome inhibitor, enrichs cellular polyubiquitinated adducts by reducing proteasomal degradation on ubiquitinated proteins (Fig 3.18A). Adding N-Ethylmaleimide (NEM) in the lysis buffer, a deubiquitinating enzyme inhibitor, further retains polyubiquitinated protein during sample preparation.

To examine the cellular effects of UbVs on HUWE1 substrates, HEK 293T cells were transfected with UbV4, HU.1, or HU.1_UbV4 fusion. An empty vector was used as a control. After being treated with MG132 (10 μM), the cells were harvested using NEM to prevent deubiquitination and then subjected to western blotting. Untreated transfected cells were used to act as a control. Western blot was performed to examine the total cellular level of the HUWE1 substrates, p53 (Chen et al., 2005) and PARP1 (Data not published). Both p53 and PARP1 blots

were presented at high and low exposure to better represent the Ub modified and unmodified proteins. The results showed that the MG132 has stabilized Ub modified p53 and PARP1 (Fig 3.18B lane 1-6). UbVs mildly increases Ub modified p53 compared to the untreated samples. UbV4 and HU.1 mildly stabilize p53 and PARP1 in the treated samples. Also, HU.1_UbV4 strongly stabilizes p53 and PARP1 in the treated samples. However, in the untreated sample, there are no differences.

Overall, the western blot shows that moderate effects of UbVs on the cellular HUWE1 substrate p53 and PARP1. However, more research is needed to further investigate the modulatory effect on HUWE1.

# Chapter 4: Discussion and Future Directions

Over the last decade, phage display-based protein engineering has been used to create protein probes and modulators for components of the UPS network. Various UbVs have been developed as tools to target and modulate specific domains or proteins of interest, such as DUBs and E3 ligases.

HUWE1 is a HECT E3 ligase that plays a critical role in the cell and mutations of HUWE1 have been associated with XLID. While the mutations that lead to XLID have been identified in HUWE1 tUBM and HECT domains, researching these domains has been difficult due to a lack of research tools. Phage-display screening has been used to develop two specific UbVs, UbV4 and HU.1. for HUWE1 tUBM and HECT domains respectively. This study characterized the biochemical properties of these two UbVs and examined their interactions with HUWE1.

The biochemical characterization conducted using BLI revealed that UbV4 exhibits the strongest binding affinity to the HUWE1 UBM domain, with an equilibrium dissociation constant ($K_d$) of 6.6 μM. This binding affinity of UbV4 towards HUWE1 UBM is 16 times stronger than its natural binder, Ub ($K_d$ = 110.6 μM).

UBM naturally binds to Ub weakly. The interaction between Ub and UBM is mediated through a continuous hydrophobic patch on Ub comprising the critical residues L8, I44 and V70 (Refer to 3.1). Upon sequence alignment with Ub, UbV4 was found to retain these conserved critical residues, with regions surrounding these critical residues becoming more hydrophobic (Fig 3.2A, B, D). This may contribute to a stronger binding affinity of UbV4 towards UBM. The caveat is that UbV4 may also bind well to other Ub-binding domains. Therefore, further testing on UbV4 interactions between the HUWE1 UBA domain or other UBDs should be conducted to address the binding specificity of UbV4 on the HUWE1 UBM domain.

Conversely, HU.1 showed a strong binding affinity for the HUWE1 HECT domain with a $K_d$ of 1.17 μM. While Ub does not bind to the HECT domain on its own (Fig 3.8), HU.1 is revealed to bind to the HECT domain with a low micromolar affinity (Fig 3.10).

When comparing HU.1 to two other E3 ligase HECT UbVs of the HECT domain with similar sequences (P1.1 & P2.3), as shown in Figure 4.1A, both UbVs had increased hydrophobic areas expanding the conserved hydrophobic patch on Ub. Furthermore, using Alphafold, the interaction of HU.1 and HECT domain was modeled (Fig 4.1C) and structurally aligned with WWP1 UbVs P1.1 and P2.3. When comparing the crystal structure of P1.1 and the HU.1 Alphafold structure against their respective E3 ligase HECT domain. HU.1 showed aromatic residues (F68, F45 & P8) in similar locations to both WWP1 UbVs P1.1 (I44, I42, F70, Y68, & L8) and P2.3 (P97, F63) aromatic residues (Fig 4.1A). These residues are directly involved in binding to their equivalent HECT domain sites (WWP1: F703, W709, and Y756) (HUWE1: Y4159 and F4181) (Fig 4.1A, B, C). Therefore, HU.1 binding sites would likely be found in the same locations as WWP1 UbVs (P1.1 and P2.3). While WWP1 UbVs interacts with WWP1 HECT domain through its HECT domain Ub exosite, the similar locations for aromatic structures on both HUWE1 UbV HU.1 and HUWE1 HECT domain suggest that HU.1 could also interact with the HUWE1 HECT domain Ub exosite (Fig 4.1B, C). To further confirm this, a structural based analysis such as NMR or co-crystallization could be carried out. Co-crystallization would also be used to determine the binding location and interaction site of each UbV.

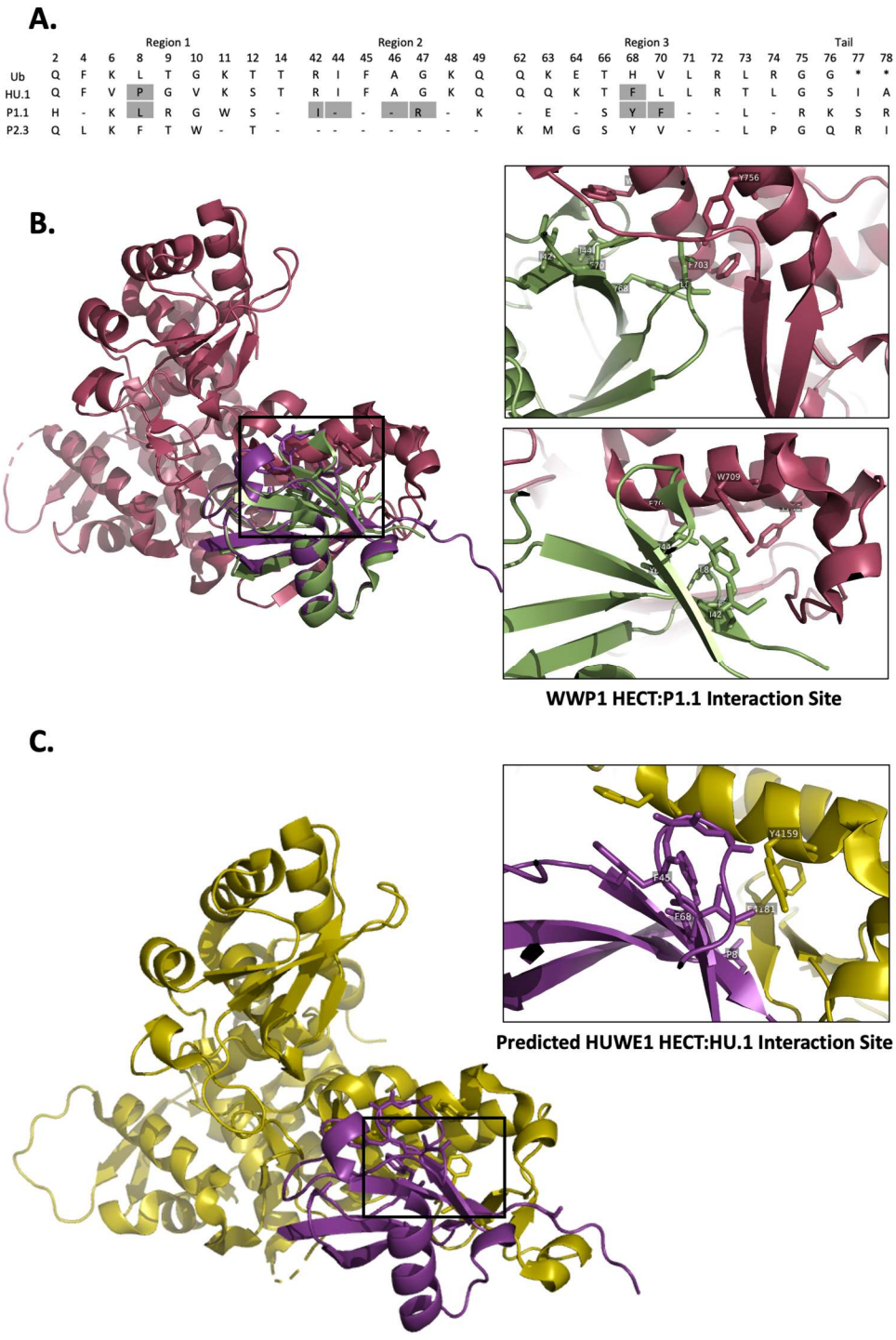


**Figure 4.1: A Potential Interaction site between HU.1 and HUWE1 HECT domain**

A) Sequence Alignment shows that most of the sequence is conserved with similar areas of interaction conserving the residue across all three UbVs hydrophobic regions.B) Structural Alignment of HU.1 (AlphaFold model) and P1.1 on WWP1 HECT: P1.1 (5HPS) structure (WWP1: Rose, P1.1: Green, HU.1: Purple) B) Possible interaction sites between HUWE1 HECT: HU.1 (HUWE1: Yellow, HU.1: Purple)

HU.1 was found to unexpectedly bind the UBM domain. HU.1 binds to the UBM domain with a $K_d$ of 20.1 μM, fivefold stronger than the UBM natural binder Ub (110.6 μM), but weaker than UbV4 (6.6. μM). Upon aligning with Ub (Refer to Fig 3.2A-E), it is apparent that HU.1, like UbV4, possesses extended hydrophobic area at the canonical interaction site of Ub. This may enable HU.1 to have stronger binding to UBM. So, HU.1 in addition to binding to HECT domain, also contains an off-target binding affinity to the HUWE1 UBM domain. This means that future research can further develop HU.1 by further mutating the sequence for improved specificity to the HUWE1 HECT domain.

Following the biochemical characterization of the interactions between UbVs and the HUWE1 proteins, these interactions were further validated in the cell. To determine whether UbV4 and HU.1 interact with HUWE1 in the cell, the study used a Co-IP to pull down the FLAG-tagged UbVs and the interacting protein HUWE1, confirming that both UbV4 and HU.1 bind to HUWE1. Limitations in this study are that the Co-IP is qualitative, as both cellular HUWE1 level and transiently expressed UbV levels affect the efficiency of pull-down.

In addition, the effect of each UbV on the endogenous HUWE1 was tested in the absence and presence of the proteasome inhibitor MG132. The results demonstrate that UbV4, HU.1 and the UbV fusion provide visible modulation to the HUWE1 function. The results showed that MG132 treatment resulted in an increase in the ubiquitinated p53 and cellular PARP1 levels in UbV4 and HU.1 or HU.1_UbV4 fusion. However, in the absence of MG132, UbV4 has no effect on p53 and PARP1.

Some limitations of the experiment arose from the variability in transfection efficiency and the transience of both UbVs expression levels in the cell. The amount of protein expressed from the transfections is not regulated across different experimental groups. Both these discrepancies

could potentially obscure subtle differences UbVs have against their controls. To rectify these limitations, UbVs can be introduced to the cells by using a lentiviral delivery system which is known as inducible expression. Each UbV expression could then be controlled and fully expressed within the cell samples, allowing for more substantial changes in each UbV modulatory effect. Overall, the study determined that UbV4 and HU.1 bind to their domain of interest biochemically and cellularly. Further structure functional analysis should be carried out to understand the role of the HUWE1 UbVs.

In addition, based on the results from this study, each HUWE1 UbV could cross-interact with HUWE1's other Ub binding motifs, UBA and UIM. This should be examined experimentally as the results would reveal whether binding interaction is specific to HUWE1 UBM and HUWE1 HECT. To address the specificity of UbV, the other cellular interacting proteins can be investigated through affinity MS. One such method is BioID. It works by fusing the target protein with a biotin-ligase that biotinylates the cellular proteins based on proximity of the target protein. All the target protein interactome can be biotinylated and identified via mass spectrometry (MS) (Samavarchi-Tehrani et al., 2018). HUWE1 UbVs can be cloned into BioID vector to fuse with a biotin ligase. Once transfected into the cell, the UbV-Biotin ligase could biotinylate UbV interacting proteins including HUWE1. This would allow us to validate UbVs binding to HUWE1 and other non-specific interactions. However, the limitation of BioID for substrate detection is that biotin ligase may biotinylate indirect or nearby interactions.

Another direction of future research could be Proteolysis-targeting Chimera (PROTAC) development. PROTAC is initially a strategy for small molecules that works by fusing a target binder and an E3 binder together. The target binder binds to the target while the E3 binder binds to the E3 ligase, which allows for the E3 to ubiquitinate the target causing Ub-mediated protein

degradation (Kelm et al., 2023). This study showed UbV4 and fusion UbV as HUWE1 binders and modulators; therefore, each UbV could be tested and designed as the E3 ligase binder for HUWE1. Future study will fuse a target binding with HUWE1 UbV and examine whether the fusion would induce targeted proteolysis.

In conclusion, the HUWE1 UbVs can strongly interact with their domains of interest and the cellular HUWE1 protein. These results support that these UbVs can act as a binding tool for targeting HUWE1 in the cell. Therefore, this study helped create and characterize an important tool in the research on HUWE1 that can potentially guide us to understand better the function of HUWE1 and HUWE1-associated XLID.

Although our research characterizes the binding and function of the HUWE1 UbVs, it remains to go further in-depth on their function before they can be used as a research tool for targeting HUWE1. Therefore, it is important to conduct further research between the HUWE1 UbVs and HUWE1. These studies may provide significant findings expanding the role of HUWE1 or help design possible treatments against HUWE1-mediated XLID.

# References:


Atsumi, Yuko, et al. “ATM and SIRT6/SNF2H mediate transient H2AX stabilization when dsbs form by blocking huwe1 to allow efficient ΓH2AX foci formation.” *Cell Reports*, vol. 13, no. 12, Dec. 2015, pp. 2728–2740, https://doi.org/10.1016/j.celrep.2015.11.054.

Berndsen, Christopher E, and Cynthia Wolberger. “New insights into ubiquitin E3 ligase mechanism.” *Nature structural & molecular biology* vol. 21,4 (2014): 301-7. doi:10.1038/nsmb.2780

Boughton, Andrew J., et al. “Branching via K11 and K48 bestows ubiquitin chains with a unique interdomain interface and enhanced affinity for proteasomal subunit RPN1.” *Structure*, vol. 28, no. 1, Jan. 2020, https://doi.org/10.1016/j.str.2019.10.008.

Brown, Nicholas G., et al. “Dual Ring E3 architectures regulate multiubiquitination and ubiquitin chain elongation by APC/c.” *Cell*, vol. 165, no. 6, 2016, pp. 1440–1453, https://doi.org/10.1016/j.cell.2016.05.037.

Brzovic, Peter S., et al. “A UBCH5/ubiquitin noncovalent complex is required for processive BRCA1-directed ubiquitination.” *Molecular Cell*, vol. 21, no. 6, Mar. 2006, pp. 873–880, https://doi.org/10.1016/j.molcel.2006.02.008.

Burschowsky, Daniel, et al. “Structural analysis of the conserved ubiquitin-binding motifs (ubms) of the translesion polymerase iota in complex with ubiquitin.” *Journal of Biological Chemistry*, vol. 286, no. 2, Jan. 2011, pp. 1364–1373, https://doi.org/10.1074/jbc.m110.135038.

Chen, Xiaoying, et al. “Fusion protein linkers: Property, design and functionality.” *Advanced Drug Delivery Reviews*, vol. 65, no. 10, 2013, pp. 1357–1369, https://doi.org/10.1016/j.addr.2012.09.039.

Chen, Yun-Ching, et al. “Generation and characterization of monoclonal antibodies against dengue virus type 1 for epitope mapping and serological detection by epitope-based peptide antigens.” *Clinical and Vaccine Immunology*, vol. 14, no. 4, 2007, pp. 404–411, https://doi.org/10.1128/cvi.00249-06.

Chen D, Kon N, Li M, Zhang W, Qin J, Gu W. “ARF-BP1/mule is a critical mediator of the ARF tumor suppressor”. *Cell*, vol 121, no. 7, 2005, pp. 1071–1083. https://doi.org/10.1016/j.cell.2005.03.037

Ciechanover, A, and A L Schwartz. “The ubiquitin-proteasome pathway: the complexity and myriad functions of proteins death.” *Proceedings of the National Academy of Sciences of the United States of America* vol. 95,6 (1998): 2727-30. doi:10.1073/pnas.95.6.2727

Deng, Lu, et al. “The Role of Ubiquitination in Tumorigenesis and Targeted Drug Discovery.” *Signal Transduction and Targeted Therapy*, vol. 5, no. 1, 29 Feb. 2020, doi:10.1038/s41392-020-0107-0.

Dikic, Ivan, et al. “Ubiquitin-binding domains — from structures to functions.” *Nature Reviews Molecular Cell Biology*, vol. 10, no. 10, 2009, pp. 659–671, https://doi.org/10.1038/nrm2767.

Ernst, Andreas, et al. “A strategy for modulation of enzymes in the ubiquitin system.” *Science*, vol. 339, no. 6119, 2013, pp. 590–595, https://doi.org/10.1126/science.1230161.

Forget, Antoine et al. “Shh signaling protects Atoh1 from degradation mediated by the E3 ubiquitin ligase Huwe1 in neural precursors.” *Developmental cell* vol. 29,6 (2014): 649-61. doi:10.1016/j.devcel.2014.05.014

French, Michael E et al. “Regulation of the RSP5 ubiquitin ligase by an intrinsic ubiquitin-binding site.” *The Journal of biological chemistry* vol. 284,18 (2009): 12071-9. doi:10.1074/jbc.M901106200

Friez, Michael J, et al. “HUWE1 mutations in Juberg-Marsidi and Brooks Syndromes: The results of an X-chromosome exome sequencing study.” *BMJ Open*, vol. 6, no. 4, 2016, https://doi.org/10.1136/bmjopen-2015-009537.

George, Arlene J., et al. “A comprehensive atlas of E3 ubiquitin ligase mutations in neurological disorders.” *Frontiers in Genetics*, vol. 9, 2018, https://doi.org/10.3389/fgene.2018.00029.

Gibson, Daniel G. “Enzymatic assembly of overlapping DNA fragments.” *Methods in enzymology* vol. 498 (2011): 349-61. doi:10.1016/B978-0-12-385120-8.00015-2

Gui, Weijun, et al. “Chemical methods for protein site-specific ubiquitination.” *RSC Chemical Biology*, vol. 2, no. 2, 2021, pp. 450–467, https://doi.org/10.1039/d0cb00215a.

Hunkeler, Moritz, et al. “Solenoid architecture of HUWE1 contributes to ligase activity and substrate recognition.” *Molecular Cell*, vol. 81, no. 17, 2021, https://doi.org/10.1016/j.molcel.2021.06.032.

Ikeda, Fumiyo, and Ivan Dikic. “Atypical ubiquitin chains: New Molecular Signals.” *EMBO Reports*, vol. 9, no. 6, 2008, pp. 536–542, https://doi.org/10.1038/embor.2008.93.

Jumper, John, et al. “Highly accurate protein structure prediction with alphafold.” *Nature*, vol. 596, no. 7873, 2021, pp. 583–589, https://doi.org/10.1038/s41586-021-03819-2.

Kanayama, Atsuhiro, et al. “Tab2 and tab3 activate the NF-KB pathway through binding to polyubiquitin chains.” *Molecular Cell*, vol. 15, no. 4, Aug. 2004, pp. 535–548, https://doi.org/10.1016/j.molcel.2004.08.008.

Kao, Shih-Han, et al. “Ubiquitination by Huwe1 in tumorigenesis and beyond.” *Journal of Biomedical Science*, vol. 25, no. 1, 2018, https://doi.org/10.1186/s12929-018-0470-0.

Kathman, Stefan G et al. “A Small Molecule That Switches a Ubiquitin Ligase From a Processive to a Distributive Enzymatic Mechanism.” *Journal of the American Chemical Society* vol. 137,39 (2015): 12442-5. doi:10.1021/jacs.5b06839

Kelm, Jeremy M., et al. “PROTAC’ing Oncoproteins: Targeted protein degradation for cancer therapy.” *Molecular Cancer*, vol. 22, no. 1, 2023, https://doi.org/10.1186/s12943-022-01707-5.

Kempeni, J. “Preliminary results of early clinical trials with the fully human anti-TNFalpha monoclonal antibody D2E7.” *Annals of the Rheumatic Diseases*, vol. 58, no. Supplement 1, 1 Nov. 1999, pp. i70–i72, https://doi.org/10.1136/ard.58.2008.i70.

Kim, Hyung Cheol, et al. “Structure and function of a HECT domain ubiquitin-binding site.” *EMBO Reports*, vol. 12, no. 4, 2011, pp. 334–341, https://doi.org/10.1038/embor.2011.23.

Koellhoffer, Jayne F., et al. “Two synthetic antibodies that recognize and neutralize distinct proteolytic forms of the ebola virus envelope glycoprotein.” *ChemBioChem*, vol. 13, no. 17, 2012, pp. 2549–2557, https://doi.org/10.1002/cbic.201200493.

Laplantine, E, et al. “Nemo specifically recognizes K63-linked poly-ubiquitin chains through a new bipartite ubiquitin-binding domain.” *The EMBO Journal*, vol. 28, no. 19, 17 Sept. 2009, pp. 2885–2895, https://doi.org/10.1038/emboj.2009.241.

Leszczynska, Katarzyna B., et al. “Hypoxia-induced p53 modulates both apoptosis and radiosensitivity via akt.” *Journal of Clinical Investigation*, vol. 125, no. 6, 11 May 2015, pp. 2385–2398, https://doi.org/10.1172/jci80402.

Lorenz, Sonja. “Structural mechanisms of HECT-type ubiquitin ligases.” *Biological Chemistry*, vol. 399, no. 2, 2017, pp. 127–145, https://doi.org/10.1515/hsz-2017-0184.

Lu, Ruei-Min, et al. “Development of therapeutic antibodies for the treatment of diseases.” *Journal of Biomedical Science*, vol. 27, no. 1, 2020, https://doi.org/10.1186/s12929-019-0592-z.

Moortgat, Stéphanie, et al. “Huwe1 variants cause dominant X-linked intellectual disability: A clinical study of 21 patients.” *European Journal of Human Genetics*, vol. 26, no. 1, 2017, pp. 64–74, https://doi.org/10.1038/s41431-017-0038-6.

Ogunjimi, Abiodun A., et al. “The ubiquitin binding region of the SMURF HECT domain facilitates polyubiquitylation and binding of ubiquitylated substrates.” *Journal of Biological Chemistry*, vol. 285, no. 9, 2010, pp. 6308–6315, https://doi.org/10.1074/jbc.m109.044537.

Park, Mi, and Jin Hong. “Roles of NF-KB in Cancer and Inflammatory Diseases and Their Therapeutic Approaches.” *Cells*, vol. 5, no. 2, 29 Mar. 2016, p. 15, doi:10.3390/cells5020015.

Pickart, Cecile M., and Michael J. Eddins. “Ubiquitin: Structures, functions, Mechanisms.” *Biochimica et Biophysica Acta (BBA) - Molecular Cell Research*, vol. 1695, no. 1–3, 2004, pp. 55–72, https://doi.org/10.1016/j.bbamcr.2004.09.019.

Ponsard, Isabelle, et al. “Selection of metalloenzymes by catalytic activity using phage display and catalytic elution.” *ChemBioChem*, vol. 2, no. 4, 2001, pp. 253–259, https://doi.org/10.1002/1439-7633(20010401)2:4<253::aid-cbic253>3.0.co;2-6.

Prezzi, C, et al. “Selection of antigenic and immunogenic mimics of hepatitis C virus using Sera from patients.” *The Journal of Immunology*, vol. 156, no. 11, 1996, pp. 4504–4513, https://doi.org/10.4049/jimmunol.156.11.4504.

Pruneda, Jonathan N., et al. “Ubiquitin in Motion: Structural Studies of the Ubiquitin-conjugating enzyme∼ubiquitin conjugate.” *Biochemistry*, vol. 50, no. 10, 2011, pp. 1624–1633, https://doi.org/10.1021/bi101913m.

Qi, Chen-Feng, et al. “Characterization of ARF-BP1/huwe1 interactions with CTCF, MYC, arf and p53 in Myc-driven B cell neoplasms.” *International Journal of Molecular Sciences*, vol. 13, no. 5, 2012, pp. 6204–6219, https://doi.org/10.3390/ijms13056204.

Samavarchi-Tehrani, Payman, et al. “A versatile lentiviral delivery toolkit for proximity-dependent biotinylation in diverse cell types.” *Molecular & Cellular Proteomics*, vol. 17, no. 11, 2018, pp. 2256–2269, https://doi.org/10.1074/mcp.tir118.000902.

Shah, Naman B., and Thomas M. Duncan. “Bio-layer interferometry for measuring kinetics of protein-protein interactions and allosteric ligand effects.” *Journal of Visualized Experiments*, no. 84, 2014, https://doi.org/10.3791/51383.

Smith, Geoffrey P, et al. “Small binding proteins selected from a combinatorial repertoire of knottins displayed on phage.” *Journal of Molecular Biology*, vol. 277, no. 2, 1998, pp. 317–332, https://doi.org/10.1006/jmbi.1997.1621.

Soboleva, Tatiana A., and Rohan T. Baker. "Deubiquitinating enzymes: their functions and substrate specificity." *Current Protein and Peptide Science* 5.3 (2004): 191-200.

Srivastava, Anshika, et al. “Histone H2A monoubiquitination in neurodevelopmental disorders.” *Trends in Genetics*, vol. 33, no. 8, Aug. 2017, pp. 566–578, https://doi.org/10.1016/j.tig.2017.06.002.

Stewart, Mikaela D, et al. “E2 enzymes: More than just middle men.” *Cell Research*, vol. 26, no. 4, 22 Mar. 2016, pp. 423–440, https://doi.org/10.1038/cr.2016.35.

Tencer, Adam H., et al. “Divergence in Ubiquitin Interaction and catalysis among the ubiquitin-specific protease family deubiquitinating enzymes.” *Biochemistry*, vol. 55, no. 33, 2016, pp. 4708–4719, https://doi.org/10.1021/acs.biochem.6b00033.

Teyra, Joan, et al. “Structural and functional characterization of Ubiquitin variant inhibitors of USP15.” *Structure*, vol. 27, no. 4, 2019, https://doi.org/10.1016/j.str.2019.01.002.

Toma-Fukai, Sachiko, and Toshiyuki Shimizu. “Structural diversity of Ubiquitin E3 ligase.” *Molecules*, vol. 26, no. 21, 2021, p. 6682, https://doi.org/10.3390/molecules26216682.

Van Wijk, Sjoerd JL, et al. “Visualizing ubiquitination in Mammalian Cells.” *EMBO Reports*, vol. 20, no. 2, 2019, https://doi.org/10.15252/embr.201846520.

Veggiani, Gianluca, et al. “Panel of engineered ubiquitin variants targeting the family of human ubiquitin interacting motifs.” *ACS Chemical Biology*, vol. 17, no. 4, 6 Apr. 2022, pp. 941–956, https://doi.org/10.1021/acschembio.2c00089.

Wang, Xiangyi S., et al. “The unifying catalytic mechanism of the ring-between-ring E3 ubiquitin ligase family.” *Nature Communications*, vol. 14, no. 1, 2023, https://doi.org/10.1038/s41467-023-35871-z.

Weinblatt, Michael E., et al. “Adalimumab, a fully human anti–tumor necrosis factor α monoclonal antibody, for the treatment of rheumatoid arthritis in patients taking concomitant methotrexate: The armada trial.” *Arthritis & Rheumatism*, vol. 48, no. 1, 2003, pp. 35–45, https://doi.org/10.1002/art.10697.

Wertz, I. E., and V. M. Dixit. “Signaling to NF- B: Regulation by ubiquitination.” *Cold Spring Harbor Perspectives in Biology*, vol. 2, no. 3, 7 Oct. 2009, https://doi.org/10.1101/cshperspect.a003350.

Wolberger, Cynthia. “Mechanisms for regulating deubiquitinating enzymes.” *Protein Science*, vol. 23, no. 4, 2014, pp. 344–353, https://doi.org/10.1002/pro.2415.

Wu, Chien-Hsun, et al. “Advancement and applications of peptide Phage Display Technology in Biomedical Science.” *Journal of Biomedical Science*, vol. 23, no. 1, 2016, https://doi.org/10.1186/s12929-016-0223-x.

Wu, Han-Chung, et al. “Identification of B-cell epitope of Dengue virus type 1 and its application in diagnosis of patients.” *Journal of Clinical Microbiology*, vol. 39, no. 3, 2001, pp. 977–982, https://doi.org/10.1128/jcm.39.3.977-982.2001.

Yang, Quan, et al. “E3 ubiquitin ligases: Styles, structures and functions.” *Molecular Biomedicine*, vol. 2, no. 1, 2021, https://doi.org/10.1186/s43556-021-00043-2.

Zhang, Wei, et al. “System-wide modulation of HECT E3 ligases with selective ubiquitin variant probes.” *Molecular Cell*, vol. 62, no. 1, 2016, pp. 121–136, https://doi.org/10.1016/j.molcel.2016.02.005.

Zhao, Xudong, et al. “The n-myc-DLL3 cascade is suppressed by the ubiquitin ligase huwe1 to inhibit proliferation and promote neurogenesis in the developing brain.” *Developmental Cell*, vol. 17, no. 2, Aug. 2009, pp. 210–221, https://doi.org/10.1016/j.devcel.2009.07.009.

# Supplemental

Table S1: Restriction Enzyme Cloning UbV Primers

| Primer Name | Sequence |
|---|---|
| BamHI-Flag Forward primer (HU.1/UbV4) | 5’ G GCC CCG GAT CCA GAT TAC AAA GAT GAC GAT GAC AAA 3’ |
| XbaI-UbV4 Reverse primer | 5’ CCC GGG TTT TCT AGA TTA CGG ACC CCG ACC ACG AAA ACT 3’ |
| NotI-HU.1 Reverse primer | 5’ GGG CCT TGC GGC CGC CGC AAT AGA ACC AAG TGT TCT 3’ |

Table S2: Restriction Enzyme Cloning UbV Primers

| Primer Name | Sequence |
|---|---|
| BamHI-Flag Forward primer (HU.1) | 5’ GGC GCG CCA TTA ATT AAG GAT CCA GAT TAC AAA GAT GAC GAT GAC AAA ATG 3’ |
| XbaI-Ubeverse primer | 5’ AC TAT AGA ATA GGG CCC TCT AGA CTA CGG ACC CCG ACC ACG AAA ACT GAA C 3’ |
| GGGGS HU.1 Reverse primer | 5’ AGA CCC CCC CCC CCC AGA CCC CCC CCC CCC CGC AAT AGA ACC AAG TGT TCT CAA TAG AAG G 3’ |
| GGGGS UbV4 Forward primer | 5’ GGG GGG GGG GGG TCT GGG GGG GGG GGG GGTCT ATG CAG ATT TTA GTG AAA ACC ATT ACT GGG G 3’ |